On High-Frequency Sound Generated by Gust-Aerofoil Interaction in Shear Flow

Journal:	*Journal of Fluid Mechanics*
Manuscript ID:	JFM-14-S-0544.R1
mss type:	Standard
Date Submitted by the Author:	27-Oct-2014
Complete List of Authors:	Ayton, Lorna; University of Cambridge, Applied mathematics and theoretical physics Peake, Nigel; University of Cambridge, Applied mathematics & Theoretical Physics
Keyword:	Aeroacoustics < Acoustics

Under consideration for publication in J. Fluid Mech.

On High-Frequency Sound Generated by Gust-Aerofoil Interaction in Shear Flow

LORNA J. AYTON† AND N. PEAKE

Department of Applied Mathematics and Theoretical Physics, University of Cambridge, Wilberforce Road, CB3 0WA, UK

(Received 27 October 2014)

A theoretical model is constructed to predict the far-field sound generated by high-frequency gust-aerofoil interaction in steady parallel shear flow, including the effects of aerofoil thickness. Our approach is to use asymptotic analysis of the Euler equations linearised about steady parallel shear flow, in the limits of high frequency and small, but non-zero, aerofoil thickness and Mach number. The analysis splits the flow into various regions around the aerofoil; local inner regions around the leading and the trailing edges where sound is generated and scattered; a surface transition region accounting for the curvature of the aerofoil; a wake transition region downstream of the aerofoil; and an outer region through which the sound propagates to the observer. Solutions are constructed in all regions, and matched using the principle of matched asymptotic expansions to yield the first two terms in the expansion of both the amplitude and the phase of the far-field pressure. Result are computed for the particular case of scattering of a gust by a symmetric Joukowski aerofoil placed in symmetric Gaussian parallel shear flow. The introduction of mean shear is shown to have a significant effect on the far-field directivity and on the total radiated power.

1. Introduction

The fundamental problem of sound generation by aerofoils in flow is of great importance to the understanding of aircraft noise. One significant acoustic source, from within the aereongine, corresponds to blade-blade interaction, when the wakes from a forward blade row or structural element interact with a downstream blade row. This is seen to be one of the key components of the total sound levels (Peake & Parry 2012), and has received much attention. For instance, for a vortical wave (a so-called gust) interacting with a single aerofoil, computational schemes, such as those of Hixon *et al.* (2006) and Allampalli *et al.* (2009), have been developed to solve the full non-linear Navier-Stokes or Euler equations for thin aerofoils with an incident gust of low- to mid-range frequency; while analytical models include those of Myers & Kerschen (1997) and Tsai (1992) for high-frequency gust-aerofoil interaction. The latter models have been related to the noise generated by a gust interacting with a cascade of aerofoils by Peake & Kerschen (1997, 2004). These analytic models use Goldstein's rapid distortion theory formulation of the scattering problem, (Goldstein 1978). Bodony (2009) has also used Goldstein's formulation, but to develop a computational scheme for predicting noise generation by entropic disturbances interacting with a symmetric aerofoil. This is highly relevant to turbine noise. A second acoustic source connected with aerofoil-flow interaction, which has perhaps received less attention, arises from the airframe at take-off or approach conditions,

† Email address for correspondence: L.J.Ayton@damtp.cam.ac.uk

whereby the deployed wing flaps might interact with the engine exhaust flow to produce noise (Mengle *et al.* 2007; Semiletov *et al.* 2013).

In much of the work on gust-aerofoil interaction noise it is assumed that the background flow is uniform far upstream. However, it is quite possible that the background flow contains significant mean shear: in the internal aeroengine context this might be caused by the wake of a large structural element upstream, or by the non-uniform flow entering the aeroengine due to incidence or other installation effects; while in the context of flap-exhaust noise, the bypass/jet exhaust flow is highly sheared. We therefore believe that including the effects of mean shear in gust-aerofoil calculations is important. In a key paper, Goldstein (1978), the interaction of a gust in a steady two-dimensional background shear flow with a zero-thickness, zero-incidence semi-infinite flat plate is calculated for the first time. Since then, this theory has been extended in two directions. First, by Goldstein (1979) who considered the case of uni-directional, transversely-sheared mean flow carrying gusts which interact with semi-infinite flat plates, and Goldstein *et al.* (2013), who were particularly concerned with jet-edge interactions. One feature of these papers is that the base flow is parallel and does not change in the streamwise direction, so that scattering by bodies which modify the mean flow, i.e. nonzero thickness aerofoils, is not included. Second, by Atassi & Grzedzinski (1989) who allow for aerofoil thickness by considering a non-parallel potential mean flow, plus a small steady vortical perturbation. This allows them to study the interaction of gusts with a realistic aerofoil leading edge in the presence of weakly-sheared mean flow. The aim of the current paper is to extend both these strands of work by considering (weakly) non-parallel shear flow with significant mean vorticity, thereby allowing us to model noise generation by gusts interacting with a nonzero thickness aerofoil in mean flow with significant shear.

In order to be able to complete an analytically-based solution a number of assumptions are required. We will suppose that the aerofoil is thin, with thickness parameter denoted by $\epsilon \ll 1$, and that the reduced frequency of the incident gust is high, denoted by $k \gg 1$. The preferred limit $\epsilon k = O(1)$ is imposed, as in Myers & Kerschen (1997) and Tsai (1992). We also assume that the flow is relatively low speed (such as the speeds experienced during aircraft approach), with typical Mach numbers being $O(\epsilon^{1/2})$. We believe that these limitations still allow us to study cases of practical interest, especially since the high-frequency regime remains challenging for computational aeroacoustics. A significant step in our analysis involves transformation from Cartesian coordinates, (x, y), to pseudo-velocity potential and streamfunction coordinates, (ϕ, ψ), where ϕ is defined such that surfaces of constant ϕ are everywhere normal to the mean streamlines. This has the advantage that the aerofoil is mapped onto a flat plate, allowing the boundary conditions to be applied more readily. We then use the method of matched asymptotic expansions (Van Dyke 1975) to split the problem into several asymptotic regions around the aerofoil (shown in Figure 1); local inner regions which scale as $O(k^{-1})$ about the leading and trailing edges of the aerofoil; a transition region whose thickness scales as $O(k^{-1/2})$ along the upper and lower surfaces of the aerofoil accounting for the effects of aerofoil thickness; an acoustic outer region which describes the propagation into the far field; and a wake transition region of thickness $O(k^{-1/2})$ downstream. The solution is determined in each region, and matched to surrounding regions using Van Dyke's matching rule (Van Dyke 1975). Our aim is to obtain the first two terms in both the amplitude and the phase in each region.

The paper is organised as follows. In Section 2 we describe the formulation of the problem, and apply our coordinate transformation to the linearised Euler equations governing the gust-aerofoil interaction. In Section 3 we outline the method used to obtain the evolution of the gust through the shear flow; this is based on the Goldstein (1978)

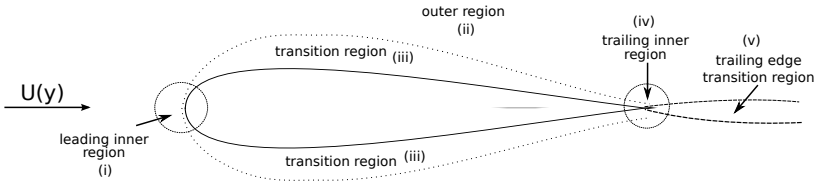

(a) In (x, y) space.

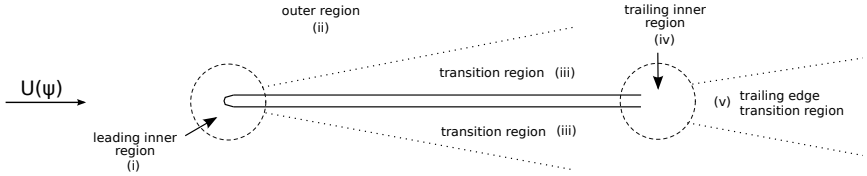

(b) In (ϕ, ψ) space.

Figure 1: Asymptotic regions around the aerofoil; leading- and trailing-edge inner regions, (i) and (iv), scale as $O(k^{-1})$, and the width of the transition regions, (iii) scales as $O(k^{-1/2})$. The outer region (ii) is $O(1)$. We solve for (i) in Section 4, then solve for a leading-edge contribution to (iii) in Section 5. Region (iii) is solved for in Section 6, and the trailing-edge contribution to (ii) along with regions (iv) and (v) are solved for in Section 7.

.

parallel-shear gust solution, but with a correction term to account for the effects of the aerofoil thickness on the steady flow. In Section 4 we solve the governing equations in the inner leading-edge region. This inner solution is then matched to a leading-edge far-field solution in Section 5, and the transition solution to account for the zero normal velocity boundary condition on the aerofoil surface is constructed in Section 6. Rescattering at the trailing edge is considered in Section 7. Results for the far-field acoustic directivity are presented in Section 8.

2. Formulation and Governing Equations

We consider a thin symmetric aerofoil aligned parallel to the x axis, with surface $y = \pm\epsilon y(x)$, $0 \leqslant x \leqslant 2$. Here, lengths have been non-dimensionalised using the aerofoil semi-chord b^* (* denotes dimensional quantities). The aerofoil sits in a mean shear flow of velocity $\boldsymbol{U}$, which is aligned parallel to the aerofoil chord at infinity (velocities are non-dimensionalised using U^*_∞, the uniform mean flow speed at infinity in the transverse direction, and we explicitly exclude the case $U^*_\infty = 0$). We work in the orthogonal (ϕ, ψ) coordinate system, where ψ is the non-dimensional mean-flow stream function and ϕ is the non-dimensional pseudo-velocity potential, chosen such that surfaces of constant ϕ and ψ are orthogonal. The origin in (ϕ, ψ) space is located at the leading edge of the aerofoil. This coordinate system has the advantage of mapping the aerofoil surface onto the flat plate $\psi = 0$, $0 \leqslant \phi \leqslant \phi_e$, where ϕ_e must be calculated from the mean-flow solution. Far upstream the steady shear flow velocity is $U_0(\psi)\boldsymbol{e}_\phi$, where $\boldsymbol{e}_\phi$ is the unit vector in the ϕ direction, and the shear profile $U_0(\psi)$ is a given function (with the property that $U_0 \to 1$ as $\psi \to \pm\infty$). The presence of the thin aerofoil distorts the incident mean flow, and we write the total mean velocity as $\left(U_0(\psi) + \epsilon q(\phi, \psi) + O(\epsilon^2)\right)\boldsymbol{e}_\phi$. The local Mach number is denoted $M(\psi)$, which takes the value M_∞ as $\psi \to \pm\infty$; in what follows we shall be

considering low Mach number flow only, with $M = O(\epsilon^{1/2})$. This means that the steady flow around the aerofoil can be determined to $O(\epsilon)$ using incompressible thin-aerofoil theory, and it follows that (see Thwaites (1960))

$$q(z) = \frac{U_0(0)}{\pi}\mathrm{Re}\left[\int_0^2 \frac{dy(x)/dx}{z-x}dx\right], \tag{2.1}$$

where $z = \phi + \mathrm{i}\psi$. Furthermore, the corrections to the otherwise uniform steady pressure, density and sound speed due to the presence of the aerofoil are of $O(\epsilon M_\infty^2) = O(\epsilon^2)$, and to $O(\epsilon)$ are therefore ignored.

Let the incident gust have typical amplitude which is much less than ϵ, allowing linearisation about the mean flow, and dimensional frequency ω^*. In what follows we non-dimensionalise time using b^*/U_∞^*, to give non-dimensional hydrodynamic frequency $\omega = \omega^* b^*/U_\infty^*$, and we also introduce the non-dimensional acoustic frequency $k = \omega M_\infty$, where $M_\infty = U_\infty^*/c_\infty^*$. We suppose k is large, with preferred limit $k = O(\epsilon^{-1})$. The unsteady velocity, pressure and density are written in the form

$$\{u, v, p, \rho\}(\phi, \psi, t) = \{u, v, p, \rho\}(\phi, \psi)\mathrm{e}^{-\mathrm{i}\omega t},$$

and we make the one further assumption that the flow is isentropic, which means that the pressure and density fluctuations are connected by $\rho = M_\infty^2 p$. The idea now is to substitute this unsteady perturbation into the equations of mass and (inviscid) momentum conservation, linearised about the steady base flow. In order to transform these equations into (ϕ, ψ) space, we use the well-known results for orthogonal curvilinear coordinates, see for example Batchelor (1967, Appendix 2). The metric elements, given by Finnigan (1983), for (ϕ, ψ)-space are

$$h_\phi = \zeta|\boldsymbol{U}| \qquad h_\psi = |\boldsymbol{U}|, \tag{2.2}$$

where ζ is defined by

$$\frac{\Omega}{|\boldsymbol{U}|^2} = \frac{\partial \log \zeta}{\partial \psi}, \tag{2.3}$$

and $\Omega = -\boldsymbol{\nabla}_{\boldsymbol{x}}^2\psi$ is the mean vorticity ($\boldsymbol{\nabla}_{\boldsymbol{x}}$ denotes the differential operator with respect to non-dimensional physical coordinates). This leads to

$$-\mathrm{i}\omega u + \zeta|\boldsymbol{U}|^2\frac{\partial u}{\partial \phi} - \Omega v + \zeta|\boldsymbol{U}|\frac{\partial p}{\partial \phi} = -u\zeta\frac{\partial}{\partial \phi}\left(\frac{|\boldsymbol{U}|^2}{2}\right), \tag{2.4a}$$

$$-\mathrm{i}\omega v + \zeta|\boldsymbol{U}|^2\frac{\partial v}{\partial \phi} + |\boldsymbol{U}|\frac{\partial p}{\partial \psi} = v\zeta\frac{\partial}{\partial \phi}\left(\frac{|\boldsymbol{U}|^2}{2}\right) - 2v\left(\Omega + \frac{\partial}{\partial \psi}\left(\frac{|\boldsymbol{U}|^2}{2}\right)\right), \tag{2.4b}$$

$$-\mathrm{i}\omega\rho + \zeta|\boldsymbol{U}|\frac{\partial u}{\partial \phi} + |\boldsymbol{U}|\frac{\partial v}{\partial \psi} + \zeta|\boldsymbol{U}|^2\frac{\partial \rho}{\partial \phi} = \frac{v}{|\boldsymbol{U}|}\left(\Omega + \frac{\partial}{\partial \psi}\left(\frac{|\boldsymbol{U}|^2}{2}\right)\right) + u\zeta\frac{\partial|\boldsymbol{U}|}{\partial \phi} \tag{2.4c}$$

for the two momentum and one mass equations respectively.

Since we are considering the case of a parallel shear flow disturbed by a thin aerofoil, we make the expansions

$$\zeta|\boldsymbol{U}|^2 = U_0(\psi) + \epsilon N_1(\phi, \psi), \tag{2.5a}$$

$$\Omega = -U_0\frac{dU_0}{d\psi} + \epsilon N_2(\phi, \psi), \tag{2.5b}$$

$$\zeta|\boldsymbol{U}| = 1 + \epsilon N_3(\phi, \psi), \tag{2.5c}$$

where the first term on the right in each case is the parallel flow result and $N_{1,2,3} = O(1)$ are the aerofoil corrections. We note immediately that introducing the thin aerofoil into

the inviscid parallel mean flow does not alter the mean vorticity, so that $N_2 \equiv 0$. However, the remaining corrections, $N_{1,3}$, are non-zero and must be determined from the solution for the mean flow. Furthermore, note that the right hand sides of (2.4) are $O(\epsilon)$, which we shall denote by $\epsilon N_{4,5,6}$ respectively. This allows us to rewrite (2.4) in the form

$$-\mathrm{i}ku + M(\psi)\frac{\partial u}{\partial \phi} + \frac{M(\psi)}{M_\infty}\frac{dM}{d\psi}v + \epsilon\sigma_1(\phi,\psi) = -M_\infty\frac{\partial p}{\partial \phi}, \tag{2.6a}$$

$$-\mathrm{i}kv + M(\psi)\frac{\partial v}{\partial \psi} + \epsilon\sigma_2(\phi,\psi) = -M(\psi)\frac{\partial p}{\partial \psi}, \tag{2.6b}$$

$$-\mathrm{i}kM_\infty p + \frac{\partial u}{\partial \phi} + \frac{M(\psi)}{M_\infty}\frac{\partial v}{\partial \psi} + M(\psi)M_\infty\frac{\partial p}{\partial \phi} + \epsilon\sigma_3(\phi,\psi) = 0, \tag{2.6c}$$

where

$$\sigma_1(\phi,\psi) = -M_\infty\left(N_4 - N_1\frac{\partial u}{\partial \phi} - N_3\frac{\partial p}{\partial \phi}\right), \tag{2.7a}$$

$$\sigma_2(\phi,\psi) = -M_\infty\left(N_5 - N_1\frac{\partial v}{\partial \phi} - q\frac{\partial p}{\partial \psi}\right), \tag{2.7b}$$

$$\sigma_3(\phi,\psi) = -\left(N_6 - N_3\frac{\partial u}{\partial \phi} - q\frac{\partial v}{\partial \psi} - N_1M_\infty^2\frac{\partial p}{\partial \phi}\right). \tag{2.7c}$$

In order to complete our solution, we introduce the Fourier transform with respect to ϕ,

$$F(\alpha,\psi) = \frac{1}{2\pi}\int_{-\infty}^{\infty}\mathrm{e}^{-\mathrm{i}\alpha\phi}f(\phi,\psi)d\phi, \tag{2.8}$$

with capital letters denoting transformed functions. Now taking the Fourier transform of (2.6) and rearranging, we obtain a single equation for the transformed pressure in the form

$$\frac{1}{M}\frac{\partial}{\partial \psi}\left(M\frac{\partial P}{\partial \psi}\right) + \frac{2\alpha}{k-\alpha M}\frac{dM}{d\psi}\frac{\partial P}{\partial \psi} + \frac{M_\infty^2}{M^2}\left((k-\alpha M)^2 - \alpha^2\right)P = \epsilon\Sigma(\alpha,\psi), \tag{2.9}$$

where

$$\Sigma(\alpha,\psi) = -\frac{\Sigma_2}{M} - \mathrm{i}(k-\alpha M)\frac{M_\infty}{M^2}\Sigma_3 - \frac{2\alpha dM/d\psi}{M(k-\alpha M)}\Sigma_2 - \frac{\mathrm{i}\alpha M_\infty}{M^2}\Sigma_1. \tag{2.10}$$

Recall that Σ_i denotes the Fourier transform of σ_i. Equations (2.6) and (2.9) are key results, and the rest of this paper is concerned with determining their solution.

3. Form of the Incident Gust

The form of the incident gust in parallel shear flow has been given by Goldstein (1978). Our flow is weakly non-parallel, thanks to the presence of the aerofoil, and this effect appears in two ways in equation (2.6) - first, in the use of (ϕ,ψ) coordinates, which captures the curvature of the mean streamlines, and second in the presence of the terms $\sigma_{1,2,3}$ representing the interaction of the unsteady flow with the non-uniform mean flow. Even so, Goldstein's method and solutions can be applied in our case, and we need only briefly outline his approach and state the key results here. Although the equations we have presented already are valid for arbitrary mean shear distributions, $M(\psi)$, at this point we restrict attention to the case in which $M(\psi)$ is a symmetric function, which will simplify both the form of the gust and our subsequent acoustic calculations. We also suppose that the shear layer has a single maximum or minimum at $\psi = 0$, which limits

the number of critical layers where $M(\psi) = k/\alpha$, and makes the construction of the gust solution easier.

Let a triple of Fourier transformed solutions to equation (2.6) be denoted $\boldsymbol{Z} = \{P, U, V\}$. Equation (2.6) has two linearly independent solutions; one of them will be denoted $\boldsymbol{Z}_1$ say, and we construct a second linearly independent solution, $\boldsymbol{Z}_{\text{out}}$ say, which has the property that it consists of only outgoing waves as $\psi \to \pm\infty$. These two solutions must typically be computed numerically for a given mean shear profile, however we shall be able to calculate an asymptotic approximation for $\boldsymbol{Z}_{\text{out}}$ which is sufficient to obtain the acoustic solution. Thanks to the symmetry of the shear layer, both solutions can be written in the form

$$\boldsymbol{Z}_*(\alpha, \psi) = \{P_*(\alpha, |\psi|), (\text{sgn}\psi)U_*(\alpha, |\psi|), V_*(\alpha, |\psi|)\}. \tag{3.1}$$

The gust solution is now written as

$$\boldsymbol{\zeta}_g(\phi, \psi)\mathrm{e}^{-\mathrm{i}wt} = \{p_g(\phi, \psi), u_g(\phi, \psi), v_g(\phi, \psi)\}\mathrm{e}^{-\mathrm{i}wt}, \tag{3.2}$$

and we simply state the Goldstein (1978) result for the transverse gust velocity v_g here,

$$\begin{aligned} v_g = &\int_{\psi}^{\infty} \mathrm{e}^{\mathrm{i}k\phi/M(\eta)}\tilde{\Omega}(\eta)\left[\frac{V_1(k/M(\eta), \psi) - \gamma(\eta)V_{\text{out}}(k/M(\eta), \psi)}{U_1(k/M(\eta), \eta)}\right] d\eta \\ &- \int_{-\infty}^{\psi} \mathrm{e}^{\mathrm{i}k\phi/M(\eta)}\tilde{\Omega}(\eta)\gamma(\eta)\frac{V_{\text{out}}(k/M(\eta), \psi)}{U_1(k/M(\eta), \eta)} d\eta \qquad \text{for} \quad \psi > 0. \end{aligned} \tag{3.3}$$

In equation (3.3) we have $\gamma(\eta) = \Gamma_+^{\pm}(k/M(\eta))$ for $\eta \gtrless 0$ with

$$\Gamma_+^{\pm}(\alpha) = \frac{P_1(\alpha, 0_{\pm})V_{\text{out}}(\alpha, 0_-) - V_1(\alpha, 0_{\pm})P_{\text{out}}(\alpha, 0_-)}{P_{\text{out}}(\alpha, 0_+)V_{\text{out}}(\alpha, 0_-) - P_{\text{out}}(\alpha, 0_-)V_{\text{out}}(\alpha, 0_+)}, \tag{3.4}$$

and η is a function defined as the inverse of $f(\psi) = k/M(\psi)$ (note that this is well-defined since we consider symmetric a shear flow with a single turning point at $\psi = 0$), so

$$\psi = \eta^{\pm}(k/M(\psi)) \qquad \text{for} \quad \psi \gtrless 0. \tag{3.5}$$

In (3.3), the function $\tilde{\Omega}(\psi)$ is an arbitrary vorticity distribution that is fixed by the form of incident gust at upstream infinity. Given the symmetry of our problem we shall choose to work solely in the upper half plane, $\psi > 0$, from this point on.

We mention that whilst the general form of the solution (3.3) is taken directly from Goldstein's work, the actual value of the solution is different, because terms dependent on $\boldsymbol{Z}_1$ and $\boldsymbol{Z}_{\text{out}}$ rely on the solutions to our perturbed governing equations, rather than Goldstein's flat-plate equations. The assumptions in Goldstein (1978) are consistent with our perturbed equations, which ensures we are able use this form of the gust solution.

At this point we will expand the unsteady flow quantities, and their Fourier transforms, in the form

$$f = f^0 + \epsilon\sqrt{k}f^1 + O(\epsilon)\ . \tag{3.6}$$

This choice of expansion is inspired by the work of Myers & Kerschen (1997) for an aerofoil in uniform flow, who showed that the leading effect of the aerofoil shape on the amplitude of the unsteady flow is to introduce an $O(\epsilon\sqrt{k})$ correction. This effect arises from the interaction between the incident gust and the large mean-flow gradients close to the leading edge (with the flow at the leading edge being represented by an inverse square-root singularity in thin aerofoil theory). This interaction produces the $O(\epsilon\sqrt{k})$ term both close to the leading edge and throughout the flow. We now expand the gust solution (3.3) in the form $v_g(\phi, \psi) = v_g^0(\phi, \psi) + \epsilon\sqrt{k}v_g^1(\phi, \psi) + O(\epsilon)$, and expressions for

$v_g^{0,1}(\phi,\psi)$ are given in Appendix A. In the next section we will describe how the gust interacts with the leading-edge region to generate sound.

4. Leading-Edge Inner Solution

Here we investigate the sound generated by the interaction of the gust with the leading edge of the aerofoil (region (i) in Figure 1). We move to a leading-edge inner coordinate system, $(\Phi,\Psi) = (k\phi, k\psi)$, recalling that $k \gg 1$ is the high-frequency parameter, and write the scattered pressure as $p_a(\Phi,\Psi) = p_a^0(\Phi,\Psi) + \epsilon\sqrt{k}p_a^1(\Phi,\Psi) + O(\epsilon)$, with the suffix $_a$ denoting that this part of the solution contains the acoustic field generated by the gust-aerofoil interaction. The leading-order solution, $p_a^0(\Phi,\Psi)$, represents the effect of the blocking of the transverse momentum of the incident gust by the solid aerofoil surface approximated as a flat plate, while the perturbation $p_a^1(\Phi,\Psi)$ represents the effects of thickness.

In the inner region the magnitude of the perturbation to the mean velocity, q, is determined by substituting inner (polar) variables into (2.1) and expanding, to give

$$q(R,\theta) = -\frac{\mathrm{i}\sqrt{k}}{2\sqrt{R}}\cos\frac{\theta}{2}\,. \tag{4.1}$$

Note how the perturbation to the mean flow, which is of size $O(\epsilon)$ in the outer region, has been promoted to size $O(\epsilon\sqrt{k})$ in the inner region, thanks to the presence of the inverse square-root singularity at the leading edge. This is what gives rise to the expansion (3.6).

4.1. *General Solution for Inner Leading-Edge Acoustic Pressure*

In this inner region it appears that the aerofoil is a semi-infinite flat plate $\Phi > 0, \Psi = 0$, and hence we use the Wiener-Hopf method (Noble 1998) to solve for the leading-edge inner acoustic solution. We write the solution as

$$p_a(\Phi,\Psi) = \mathrm{sgn}(\Psi)\int_{-\infty}^{\infty} \mathrm{e}^{\mathrm{i}\alpha\Phi/k}A(\alpha)P_{\mathrm{out}}(\alpha,|\Psi|)d\alpha, \tag{4.2a}$$

$$v_a(\Phi,\Psi) = \int_{-\infty}^{\infty} \mathrm{e}^{\mathrm{i}\alpha\Phi/k}A(\alpha)V_{\mathrm{out}}(\alpha,|\Psi|)d\alpha, \tag{4.2b}$$

demanding outgoing-wave behaviour at infinity. We also enforce the boundary conditions that $v_a = -v_g$ on $\Phi > 0, \Psi = 0$ (in order to cancel the incident gust transverse velocity on the aerofoil surface), and that the pressure is continuous across $\Psi = 0$ for $\Phi < 0$. These two conditions lead to the integral equations

$$\begin{aligned}
&\int_{-\infty}^{\infty} \mathrm{e}^{\mathrm{i}\alpha\Phi/k}A(\alpha)V_{\mathrm{out}}(\alpha,0)d\alpha = -v_g(\Phi,0) \qquad \text{for} \quad \Phi > 0\\
&\int_{-\infty}^{\infty} \mathrm{e}^{\mathrm{i}\alpha\Phi/k}A(\alpha)P_{\mathrm{out}}(\alpha,0)d\alpha = 0 \qquad\qquad\quad \text{for} \quad \Phi < 0\,.
\end{aligned} \tag{4.3}$$

The solution to this Wiener-Hopf problem is described in detail in Appendix B, and we write

$$p_a^{0,1}(\Phi,\Psi) = \int_0^{\infty} p_a^{0,1}(\Phi,\Psi|\eta)d\eta, \tag{4.4}$$

where the expression for $p_a^{0,1}(\Phi,\Psi|\eta)$ can be found in Appendix A. We have therefore found the first two terms in the inner region.

When evaluating the far-field pressure, rather than integrating over η as required by (4.4), we follow Goldstein (1978) and simply evaluate our expressions for $p(\phi,\psi|\eta)$ at

$\eta = 0$. This is motivated by the assumption that the gust vorticity distribution, $\tilde{\Omega}$, is sharply peaked at $\eta = 0$, so that the integration is dominated by the contribution from $\eta = 0$. A sharp peak of vorticity at $\eta = 0$ is characteristic of turbulent shear layers; see Goldstein (1978) for further details.

4.2. *Outer limit of the inner solution*

4.2.1. *Solution for P^0*

Taking (2.9) to $O(1)$ gives an equation for the Fourier transform of the leading-order pressure, P^0;

$$\frac{\partial^2 P^0}{\partial \psi^2} - \frac{2M'\alpha}{\alpha M - k}\frac{\partial P^0}{\partial \psi} + \frac{M'}{M}\frac{\partial P^0}{\partial \psi} + \frac{M_\infty^2}{M^2}\left[(\alpha M - k)^2 - \alpha^2\right]P^0 = 0. \tag{4.5}$$

All the terms in (4.5) balance provided $\alpha = O(k)$, and we therefore define $\beta \equiv \alpha/k$ with $\beta = O(1)$. This is a valid scaling of α in the inner region, since the Fourier phase, $-\mathrm{i}\phi\alpha$, can then be written as $-\mathrm{i}\Phi\beta$ in inner variables, allowing for $O(1)$ variations in Φ to be analysed. In inner coordinates, (4.5) becomes to leading order

$$\frac{\partial^2 P^0}{\partial \Psi^2} + \frac{M_\infty^2}{M_0^2}\left[(\beta M_0 - 1)^2 - \beta^2\right]P^0 = 0, \tag{4.6}$$

where $M_0 = M(0)$ is the Mach number in the inner region. Equation (4.6) has an outgoing-wave solution

$$P^0_{\mathrm{out}}(\alpha, \Psi) = C^0(\alpha)\exp\left[\mathrm{i}\sqrt{(1-\alpha M_0/k)^2 - (\alpha/k)^2}\frac{M_\infty}{M_0}|\Psi|\right], \tag{4.7}$$

where

$$C^0(\alpha) = c\left[\left(1 - \frac{\alpha M_0}{k}\right)^2 - \left(\frac{\alpha}{k}\right)^2\right]^{-1/4} \tag{4.8}$$

and c is an arbitrary constant. The reasons we include the factor defined in (4.8) are two-fold. First, the factor is included in order to match with the form of solution used by Goldstein (1978) in parallel shear flow - Goldstein developed a WKB solution and the factor appears there as the usual WKB amplitude. Second, the factor is included in order to recover the leading-order directivity known to be present in leading-edge scattering of both vorticity and sound - we will return to this point later in this subsection.

Taking the form of solution (4.8), substituting into (A 2*a*) and using the method of stationary phase (Bender & Orszag 1978), we find that the outer limit of the inner acoustic solution is

$$p_a^0(r,\theta|\eta) \sim -\left(\frac{\mathrm{i}}{2\pi kr}\right)^{1/2}\frac{\sin\theta \mathrm{e}^{\mathrm{i}kr\lambda_0(\theta)}}{(1-M_0^2\sin^2\theta)^{3/4}}\frac{\tilde{\Omega}(\eta)\tilde{Q}^0(\eta)M(\eta)}{1-\beta_0 M(\eta)}\frac{\kappa^0(k/M(\eta))_+ C^0(k\beta_0)}{\kappa^0(k\beta_0)_+ V^0_{\mathrm{out}}(k\beta_0,0)}, \tag{4.9}$$

where (r,θ) are polar coordinates in $(\phi,\psi)-$space centred on the leading edge. We note that the arbitrary constant, c, is cancelled out in the term C^0/V^0_{out} in light of (B 5). In (4.9) we have introduced the phase function, λ, defined as

$$\lambda(\beta, M) = \beta\cos\theta + \frac{M_\infty}{M}\sqrt{(1-M\beta)^2 - \beta^2}\,, \tag{4.10}$$

which has the point of stationary phase

$$\beta^s(M) = -\frac{1}{1-M^2}\left(M - \frac{\cos\theta}{\sqrt{\cos^2\theta + \frac{M_\infty^2}{M^2}\sin^2\theta - M_\infty^2\sin^2\theta}}\right). \tag{4.11}$$

The functions $\lambda_0(\theta)$ and $\beta_0(\theta)$ are defined as

$$\lambda_0(\theta) = \lambda(\beta_0, M_0), \qquad \beta_0 = \beta^s(M_0). \tag{4.12}$$

The steady Mach number takes the value M_0 throughout the inner region, and the phase in (4.9) is therefore given by (4.10) and (4.11) with $M = M_0$. Furthermore in (4.9), the function $\kappa_+^0(\eta)$ arises from the Wiener-Hopf solution of the inner problem, see (B 5), while the function $\tilde{Q}^0(\eta)$ appears in the form of the incident gust and is defined following equation (B 14).

We now return to the question of the choice of the factor in (4.8). We know from Tsai (1992) and Ayton & Peake (2013) that the leading-order outer solution for gust-aerofoil and sound-aerofoil interaction in uniform steady flow has directivity $\cos\theta/2$. In steady shear flow, sound is produced at the leading edge both by the scattering of the vortical gust (as in Tsai (1992)), and by the scattering of the the gust self-noise (similar to Ayton & Peake (2013)). Throughout the inner region the mean shear does not appear, and the mean flow is simply uniform with Mach number M_0, and the $\cos\theta/2$ directivity must therefore be recovered in the outer limit of the inner solution in the present problem too. In fact, our choice of $C^0(\alpha)$ gives

$$P^0 \propto \cos(\theta/2)\left(1 - M_0/2 + (3+\cos 2\theta)M_0^2/4 + O(M_0^3)\right), \tag{4.13}$$

confirming the required directivity.

4.2.2. *Solution for P^1*

Taking $O(\epsilon\sqrt{k})$ terms in (2.9) and converting to inner coordinates gives an equation for P^1;

$$\frac{\partial^2 P^1}{\partial\Psi^2} + \frac{M_\infty^2}{M_0^2}\left(1 - 2M_0\beta - \beta^2(1-M_0^2)\right)P^1 = \Sigma(\alpha,\Psi). \tag{4.14}$$

Here we have used the fact that to leading order $\Sigma(\alpha,\Psi) \equiv \sqrt{k}\Sigma(\alpha, k\psi)$, which follows from the inverse square-root singularity of the steady flow at the leading edge.

We solve (4.14) using the Green's function

$$G(\Psi,\Psi') = \frac{M_0}{2\mathrm{i}M_\infty\sqrt{1-2M_0\beta-\beta^2(1-M_0^2)}}\mathrm{e}^{\mathrm{i}\sqrt{(1-M_0\beta)^2-\beta^2}\frac{M_\infty}{M_0}|\Psi-\Psi'|}, \tag{4.15}$$

which represents the desired outgoing wave field, to yield

$$\begin{aligned} P^1_{\mathrm{out}}(k\beta,\Psi) = &\int_0^\infty \frac{M_0\mathrm{e}^{\mathrm{i}\sqrt{(1-M_0\beta)^2-\beta^2}\frac{M_\infty}{M_0}|\Psi-\Psi'|}}{2\mathrm{i}M_\infty\sqrt{(1-M_0\beta)^2-\beta^2}}\Sigma(k\beta,\Psi')d\Psi' \\ &+ C^1(\beta)\mathrm{e}^{\mathrm{i}\sqrt{(1-M_0\beta)^2-\beta^2}\frac{M_\infty}{M_0}|\Psi|}. \end{aligned} \tag{4.16}$$

From (2.10) we know that each term in $\Sigma(\alpha,\Psi)$ will have a phase function $\sqrt{(1-M_0\beta)^2-\beta^2}\frac{M_\infty}{M_0}|\Psi|$ (since each σ_i is proportional to a linear combination of u^0,v^0, and p^0), and further, since Q is symmetric and Ω is antisymmetric with respect to ψ, we know that Σ is symmetric with respect to ψ. Setting

$$\hat{\Sigma}(\alpha,\Psi) = \Sigma(\alpha,\Psi)\mathrm{e}^{-\mathrm{i}\sqrt{(1-M_0\beta)^2-\beta^2}\frac{M_\infty}{M_0}|\Psi|}, \tag{4.17}$$

so that $\hat{\Sigma}$ is phase-less in the variable Ψ, and completing the Ψ' integral in (4.16), we find that the outer limit of the inner solution is

$$P^1_{\text{out}}(k\beta, k\psi) \sim \left(d(k\beta, k\psi) + C^1(k\beta)\right) \mathrm{e}^{\mathrm{i}\sqrt{(1-M_0\beta)^2-\beta^2}\, k \frac{M_\infty}{M_0}|\psi|}, \tag{4.18}$$

where $d(k\beta, \Psi)$ is given by

$$d(k\beta, k\psi) = \frac{\mathrm{i}\hat{\Sigma}(k\beta, k\psi) M_0}{k\left((1-M_0\beta)^2 - \beta^2\right) M_\infty}. \tag{4.19}$$

Following the same arguments as in the previous subsection, we choose $C^1(k\beta) = C^0(k\beta)$, and then repeating the method of stationary phase to invert the Fourier transform yields an outer expansion for p^1_a in the form

$$\begin{aligned} p^1_a(r,\theta|\eta) \sim -\left(\frac{\mathrm{i}}{2\pi kr}\right)^{1/2} & \frac{\sin\theta \mathrm{e}^{\mathrm{i}kr\lambda_0(\theta)}}{(1-M_0^2\sin^2\theta)^{3/4}} \frac{\tilde{\Omega}(\eta)\tilde{Q}^0(\eta)M(\eta)}{1-\beta_0 M(\eta)} \frac{\kappa^0(k/M(\eta))_+ C^0(k\beta_0)}{\kappa^0(k\beta_0)_+ V^0_{\text{out}}(k\beta_0, 0)} \\ & \left[\frac{\tilde{Q}^1(\eta)}{\tilde{Q}^0(\eta)} + M'(\eta)\left(\frac{P^1_{\text{out}}(k/M(\eta),0)}{P^0_{\text{out}}(k/M(\eta),0)} - \frac{V^1_{\text{out}}(k/M(\eta),0)}{V^0_{\text{out}}(k/M(\eta),0)}\right)\right. \\ & \left. + \frac{1}{C^0(k\beta_0)}\left(d(k\beta_0, k\psi) - d(k\beta_0, 0)\right)\right], \end{aligned} \tag{4.20}$$

where β_0 and λ_0 are given in (4.12). Comparing (4.20) and (4.9), we see that p^1_a is obtained by multiplying p^0_a by the correction factor given in square brackets in (4.20). This correction factor has arisen from two separate effects; the first two sets of terms inside the square brackets in (4.20) arise from the distortion of the incident gust by the non-uniform mean flow round the aerofoil; while the third set of terms, involving the function $d(k\beta, k\psi)$, arises from the source terms in (2.9), i.e. from the interaction between the leading-order scattered field and the non-uniform mean flow near the leading edge. The correction term in (4.20) will have the important effect of introducing constructive and destructive interference between the two leading-edge fields p^0_a and p^1_a, and we return to this point in Section 8.

Note that whilst Σ, as defined in (2.10), has appeared in our solution through equation (4.19), we only need to calculate the inner limit of Σ in order to establish (4.20). This is in exact parallel to the work of Myers & Kerschen (1997) and Tsai (1992), who found that in a uniform stream the leading contribution of the volume terms only appears close to the leading edge where the mean flow gradients are large. Therefore, to calculate the outer limit of the inner leading-edge solution we only need to find the correction terms $N_i, i = 1, .., 6$ appearing in equation (2.6) close to the aerofoil. We first note that, since $U = U_0(\psi) + \epsilon q(\phi, \psi)$, we have

$$N_1 = q + U_0 N_3, \tag{4.21}$$

while by using (2.3) we obtain the relation

$$\frac{q}{U_0^2}\frac{dU_0}{d\psi} + \frac{\partial q}{\partial \psi}\frac{1}{U_0} = \frac{\partial N_3}{\partial \psi}. \tag{4.22}$$

In the leading-edge inner region, equation (4.22) can be integrated to yield

$$N_3 = \frac{q}{U_0(0)}, \tag{4.23}$$

where an arbitrary function of ϕ has been set to zero to ensure consistency with $N_2 = 0$. It therefore follows that $N_1 = 2q$. The quantities $N_{4,5,6}$ can be found immediately from

expressions we have obtained for ζ, q and Ω, with

$$N_4 = u_0 \frac{\partial q}{\partial \phi}, \qquad N_5 = v_0 \frac{\partial q}{\partial \phi}\left(1 - 2U_0(0)\right), \qquad N_6 = \frac{\partial q}{\partial \phi}\left(v_0 + \frac{u_0}{U_0(0)}\right), \tag{4.24}$$

again all evaluated in the inner region.

In summary, we have determined the first two terms in the outer limit of the inner pressure field, given by equations (4.9) and (4.20) which are integrated in (4.4). As mentioned previously, we assume the vorticity distribution is sharply peaked at $\eta = 0$, allowing us to use Laplace's method to evaluate (4.4). We will write the sum of these two terms in the form

$$\frac{\mathcal{P}_l(\theta)}{\sqrt{kr}} \exp(\mathrm{i}kr\lambda(\beta_0)) \,, \tag{4.25}$$

and we will match this expression onto the outer solution in the next section.

5. Leading-Edge Outer Solution

In this section we determine the leading-edge contribution to the acoustic pressure in the far field. The sound generated by the gust-aerofoil interaction in the leading-edge inner region, as determined in the previous section, propagates through the outer region, denoted by region (ii) in Figure 1, and is distorted by the mean shear. The acoustic field of a point source in a mean shear has been determined by Durbin (1983), and we use those results here.

The outer solution which matches with the outer limit of the inner solution takes the form

$$p_l = \frac{s(r,\theta)\mathcal{P}_l(\theta)}{\sqrt{kr}} \exp(\mathrm{i}k\varrho^0 + \mathrm{i}k\epsilon\varrho^1) \,. \tag{5.1}$$

Here $\mathcal{P}_l(\theta)$ is the directivity of the inner solution as it emerges into the outer region, as defined in (4.25). The factor $s(r,\theta)$ is the scaling factor derived by Durbin (1983) to account for the distortion of the pressure amplitude due to variation in the ray tube area through the shear, and is given by

$$s(r,\theta) = \left(\frac{1-M_0^2}{1-M_0^2\sin^2\theta}\right)^{1/4} \left(\frac{M - M\frac{\partial \sigma_1}{\partial \phi}}{M_0 - M_0\left.\frac{\partial \sigma_1}{\partial \phi}\right|_{r\to 0}}\right) \left(\lambda\sqrt{1-M_0^2}\cos\mu' \frac{\partial \mu'}{\partial \mu}\right)^{-1/2} . \tag{5.2}$$

In (5.2), μ is the local ray angle (and μ' is its value at the leading edge) - see Durbin (1983) equation (26b) - while λ is the local ray speed - see Durbin (1983), following his equation (16). A factor in $s(r,\theta)$ involving the local sound speed, present in Durbin (1983), has been set to unity for our low Mach number flow. Note that $s(r,\theta) \to 1$ as $r \to 0$, while in the limit $r \to \infty$, $s(r,\theta) \to s(\theta)$, where the latter can easily be calculated from (5.2).

We determine the first two terms phase terms, $\varrho^{0,1}$, in (5.1) by substituting the ansatz (5.1) into an equation formed by rearranging (2.6) into a single equation for p. We then take the real parts of the resulting equation at the first two asymptotic orders to form two eikonal equations for $\varrho^{0,1}$. In what follows we will only require the acoustic pressure in the far field (i.e. $r \to \infty$), and we therefore write down expressions for the phase terms which are valid there. The first eikonal equation can easily be solved to give the first phase term in the form

$$\varrho^0 = kr\lambda(\beta_\infty, M_\infty) \equiv kr\lambda_\infty(\theta), \tag{5.3}$$

where $\beta_\infty = \beta^s(M_\infty)$.

The second eikonal equation is more complicated, since it includes contributions from the terms $\sigma_{1,2,3}$ in (2.6), which arise from the interaction between the leading-order unsteady flow and the steady-flow non-uniformity caused by the presence of the aerofoil. After some algebra we find that the second eikonal equation is

$$\frac{\partial \varrho^1}{\partial \phi} + \frac{\partial \varrho^1}{\partial \psi} = \frac{1}{2} L(\phi, \psi), \tag{5.4}$$

where the term $L(\phi, \psi)$ involves the terms $\sigma_{1,2,3}$. Specifically, we introduce the quantity

$$M_\infty \sigma(\phi, \psi) = -\mathrm{i}k\sigma_3 + M\frac{\partial \sigma_3}{\partial \phi} - \frac{\partial \sigma_1}{\partial \phi} - \frac{M}{M_\infty}\frac{\partial \sigma_2}{\partial \psi}, \tag{5.5}$$

which, in the light of (5.1), to leading-order in the outer region takes the form

$$\sigma(\phi, \psi) = \frac{k^{3/2} L(\phi, \psi)\mathcal{P}(\theta)s(\theta)}{\sqrt{r}} \mathrm{e}^{\mathrm{i}k\varrho^0(r,\theta) + ik\epsilon\varrho^1(r,\theta)}, \tag{5.6}$$

where

$$L(\phi, \psi) = \left(\frac{\partial \varrho^0}{\partial \phi}\right)^2 \left[\frac{q}{U_0} + \int_\psi^\infty \frac{2qU_0'(\psi')}{U_0(\psi')^2} d\psi'\right] + q\left(\frac{\partial \varrho^0}{\partial \psi}\right)^2. \tag{5.7}$$

The solution of (5.4) can now be determined using the method of characteristics in the form

$$\varrho^1(r, \theta) = \frac{1}{2}\int_0^{\phi+\psi} L(\chi, \psi) d\chi, \tag{5.8}$$

where $\chi = \phi + \psi$ is the characteristic variable.

We have therefore completed the construction of the far-field solution for the noise emanating from the leading edge of the aerofoil, and we write finally the acoustic pressure as $r \to \infty$ in the form

$$\frac{D_l(\theta)}{\sqrt{kr}} \exp\left(\mathrm{i}kr\lambda_\infty(\theta) + \frac{1}{2}\mathrm{i}k\epsilon \int_0^{\phi+\psi} L(\chi, \psi) d\chi\right), \tag{5.9}$$

where the leading-edge directivity is given by $D_l(\theta) = \mathcal{P}_l(\theta)s(\theta)$. We emphasise that this solution is not valid in the mid field, where the mean flow is sheared; it is only valid in the far field, where $M \approx M_\infty$.

6. Leading-Edge Transition Solution

The transition solution (region (iii) in Figure 1) accounts for the curvature of the surface of the aerofoil, in a very similar manner to the case of uniform flow considered by Tsai (1992), and corrects for the boundary condition of zero normal velocity on the aerofoil surface that is violated by the leading-edge outer solution. We therefore suppose the transition solution takes the form

$$p_{ltr} = \epsilon G(\phi, \xi) \mathrm{e}^{\frac{\mathrm{i}k\phi}{1+M} + \frac{1}{2}\mathrm{i}k\epsilon \int_0^\phi L(\phi', 0) d\phi'}, \tag{6.1}$$

where $\xi = \sqrt{k}\psi$ is the transition-region coordinate above the aerofoil in the direction normal to the surface. The choice of phase in (6.1) arises from taking $\theta = 0$ (equivalently $\psi = 0$) in (5.3 and 5.8).

In the transition region the leading-order expansion of (2.6) tells us that $G(\phi, \xi)$ must

satisfy

$$\frac{M^2}{M_\infty^2}\frac{\partial^2 G}{\partial \xi^2} + 2\mathrm{i}\frac{\partial G}{\partial \phi} = 0, \tag{6.2}$$

subject to boundary condition

$$-\epsilon\sqrt{k}\frac{\partial G}{\partial \xi}\mathrm{e}^{\frac{\mathrm{i}k\phi}{1+M}+\frac{1}{2}\mathrm{i}k\epsilon\int_0^\phi L(\phi,0)d\phi}\bigg|_{\xi=0} = -\left.\frac{\partial p_l}{\partial \psi}\right|_{\psi=0}, \tag{6.3}$$

which enforces zero total normal velocity on the aerofoil surface. We now take the Laplace transform of (6.2) with respect to ϕ, denoted by

$$\tilde{G}(S,\xi) = \int_0^\infty G(\phi,\xi)e^{-S\phi}d\phi, \tag{6.4}$$

to find that

$$\tilde{G}(S,\xi) = B(S)\mathrm{e}^{-\mathrm{e}^{-\pi\mathrm{i}/4}\sqrt{2S}\frac{M_\infty}{M}\xi}, \tag{6.5}$$

where

$$B(S) = \frac{\mathrm{e}^{3\mathrm{i}\pi/4}}{2\sqrt{2S}}\int_0^\infty \frac{\mathrm{e}^{-S\phi}}{\sqrt{\phi}}s(\phi,0)\mathcal{P}(\phi,0)\left(L(\phi,0)+\int_0^\phi \left.\frac{\partial L(\phi'+\psi,\psi)}{\partial\psi}\right|_{\psi=0}d\phi'\right)d\phi. \tag{6.6}$$

This Laplace transform can be inverted numerically to determine the transition solution.

We mention briefly here that the terms $\sigma_{1,2,3}$ in (2.6) occur at higher order and do not appear in this transition solution explicitly, although they do appear implicitly through the forcing provided by the outer solution in (6.3). Physically this is because the dominant effects of curvature arise in the leading-edge inner region, where the aerofoil is most curved, and not along the upper and lower arcs of the aerofoil.

The total far-field acoustic pressure emanating from the leading edge is given as a sum of the outer field determined in the previous section and the transition solution determined in this section. The transition solution does not appear directly in the acoustics (note from (6.5) that the transition solution decays exponentially in the transverse direction away from the aerofoil surface). It does, however, introduce a pressure discontinuity across the aerofoil, which must be corrected downstream of the trailing edge across the wake. This is done by the introduction of trailing-edge inner and transition solutions, and the inner solution matches onto an outgoing trailing-edge acoustic field. This is described in the next section.

7. Trailing-Edge Inner and Outer Solutions

Here we determine the solution in the trailing-edge inner region and the trailing-edge contribution to the outer region, denoted by (iv) and (ii) in Figure 1 respectively. The transition solution in the wake (region (v) in Figure 1) is not required for the acoustic far field, and is very similar to solutions found in uniform flow by Myers & Kerschen (1997) and Tsai (1992), and will therefore not be presented here.

We shift coordinates to be aligned with the trailing edge, defining (ϕ_t, ψ_t) such that $(\phi,\psi) = (2+\phi_t+\epsilon\alpha_t, \psi_t)$. Here $\alpha_t = O(1)$ arises from the effect of thickness during the mapping of coordinates from physical space to (ϕ,ψ)-space. By observing (2.1), α_t can be calculated in much the same way as was done by Tsai (1992) for uniform flow. The transverse velocity of the incident gust solution at the trailing edge is still given by (A 1).

7.1. *Trailing-Edge Inner Solution*

We move to inner trailing-edge coordinates, $(\Phi_t, \Psi_t) = k(\phi_t, \psi_t)$. The trailing-edge inner acoustic solution, equivalent to (4.2), satisfies a dual integral equation equivalent to (4.3), which is

$$\int_{-\infty}^{\infty} \mathrm{e}^{\mathrm{i}\alpha\Phi_t/k} A(\alpha) P_{\mathrm{out}}(\alpha, 0) d\alpha = -\Delta p(\Phi_t)/2 \quad \Phi_t > 0, \tag{7.1a}$$

$$\int_{-\infty}^{\infty} \mathrm{e}^{\mathrm{i}\alpha\Phi_t/k} A(\alpha) V_{\mathrm{out}}(\alpha, 0) d\alpha = -v_g(\Phi_t, 0) \quad \Phi_t < 0. \tag{7.1b}$$

Here all functions are written in terms of trailing-edge coordinates, α is redefined accordingly as the Fourier transform variable with respect to ϕ_t and $\Delta p(\Phi_t)$ is the inner approximation for the pressure jump across the trailing edge generated by the leading-edge solution. We separate the required inner solution, $p_a(\Phi_t, \Psi_t)$, into a term that corrects the pressure jump across the trailing edge, $p_{a,p}$, and a term that corrects for the zero normal velocity condition on the surface of the aerofoil, $p_{a,H}$. Using the notation from (4.2), we require

$$\int_{-\infty}^{\infty} \mathrm{e}^{\mathrm{i}\alpha\Phi_t/k} A_p(\alpha) P_{\mathrm{out}}(\alpha, 0) d\alpha = -\Delta p(\Phi_t)/2 \quad \Phi_t > 0, \tag{7.2a}$$

$$\int_{-\infty}^{\infty} \mathrm{e}^{\mathrm{i}\alpha\Phi_t/k} A_p(\alpha) V_{\mathrm{out}}(\alpha, 0) d\alpha = 0 \quad \Phi_t < 0, \tag{7.2b}$$

and

$$\int_{-\infty}^{\infty} \mathrm{e}^{\mathrm{i}\alpha\Phi_t/k} A_H(\alpha) P_{\mathrm{out}}(\alpha, 0) d\alpha = 0 \quad \Phi_t > 0, \tag{7.3a}$$

$$\int_{-\infty}^{\infty} \mathrm{e}^{\mathrm{i}\alpha\Phi_t/k} A_H(\alpha) V_{\mathrm{out}}(\alpha, 0) d\alpha = -v_g(\Phi_t, 0) \quad \Phi_t < 0. \tag{7.3b}$$

The solution of (7.2) and (7.3) is obtained using identical methods to those used at the leading edge in Section 4, and is presented in Appendix C. We use the solutions for $P_{\mathrm{out}}^{0,1}$ as previously obtained in Section 4.2, but translated to the trailing-edge inner coordinate system. Taking the outer limit of the inner solutions, (C 1), and using the method of steepest descents yields

$$\begin{aligned} p_a^t(r_t, \theta_t | \eta_t) \sim & \left(\frac{\mathrm{i}}{2\pi k r_t}\right)^{1/2} \frac{\kappa_t^0(k\beta_{t0})_- \sin\theta_t}{(1 - M_0^2 \sin^2\theta_t)^{3/4}} \frac{\mathrm{e}^{\mathrm{i}kr_t\lambda_{t\,0}(\theta_t)}}{1 - \beta_{t0} M(\eta_t)} \frac{C^0(k\beta_{t0})\tilde{\Omega}(\eta_t)\tilde{Q}^0(\eta_t) M(\eta_t)}{\kappa_t^0(k/M(\eta_t))_- V_{\mathrm{out}}^0(k\beta_{t0}, 0)} \\ & \left[1 + \epsilon\sqrt{k}\left\{\frac{\tilde{Q}^1(\eta_t)}{\tilde{Q}^0(\eta_t)} + M'(\eta_t)\left(\frac{P_{\mathrm{out}}^1(k/M(\eta_t), 0)}{P_{\mathrm{out}}^0(k/M(\eta_t), 0)} - \frac{V_{\mathrm{out}}^1(k/M(\eta_t), 0)}{V_{\mathrm{out}}^0(k/M(\eta_t), 0)}\right)\right.\right. \\ & \left.\left. + \frac{d_t(k\beta_{t0}, \Psi_t) - d_t(k\beta_{t0}, 0)}{C^0(k\beta_{t0})}\right\}\right] \\ & + \left(\frac{\mathrm{i}}{2\pi k r_t}\right)^{1/2} \frac{\kappa_t^0(k\beta_{t0})_- \sin\theta_t \mathrm{e}^{\mathrm{i}kr_t\lambda_{t\,0}(\theta_t)}}{(1 - M_0^2 \sin^2\theta_t)^{3/4}} \frac{G_{t,p}(k\beta_{t0}) P_{\mathrm{out}}^0(k\beta_{t0})}{V_{\mathrm{out}}^0(k\beta_{t0})} \end{aligned} \tag{7.4}$$

as $kr_t \to \infty$, where $\lambda_{t\,0}$ is the trailing-edge equivalent of λ_0, and β_{t0} is the trailing-edge equivalent of β_0 as defined in (4.12). The final term in (7.4) is in fact $O(k^{-1})$ due to the scaling of the pressure jump term $G_{t,p}$. It will be shown later that the term involving $d_t(k\beta_{t0}, \Psi_t)$ in (7.4) is negligible to the orders retained here since in the trailing-edge region the terms σ_i in (2.6) are negligible (because there is less curvature of the streamlines at the trailing edge than at the leading edge for the aerofoils we wish to consider,

such as the Joukowski aerofoil or the NACA 4-digit series of aerofoils). The choice of C^0 is again given by (4.8), which now ensures that the trailing-edge inner solution has a $\sin\theta/2$ directivity pattern. This is the same directivity pattern found for sound- and gust-aerofoil interaction in steady uniform flow in Ayton & Peake (2013) and Myers & Kerschen (1997) respectively. Once again we know that the shear flow directivity pattern should match the uniform flow directivity pattern to leading order, since in the trailing-edge inner region the aerofoil only experiences the local Mach number M_0. Note that at the trailing edge we only need a match to $O(M_0) = O(\sqrt{\epsilon})$ (as opposed to $O(M_0^2) = O(\epsilon)$ required for the inner leading-edge solution, (4.13)) since the trailing-edge scattered field of gust-aerofoil interaction is $O(k^{-1/2})$ smaller than the leading-edge field, and in the uniform limit the first two terms in (7.4) tend to zero since $(\kappa_t^0(k/M(\eta_t))_-)^{-1} \to 0$ as $M(\psi) \to M_0$.

The terms in square brackets in (7.4) represent the scattering of the pressure associated purely with the gust in the shear flow by the aerofoil (in uniform flow a gust is pressure-free, and these terms vanish). Whilst the contribution of these terms appears to be the same order as the contribution of the leading-edge solution, (4.9), we in fact find that it is at least $O(M)$ smaller due to $\kappa_t^0(k/M(\eta_t))_-$ having a singularity at $\eta_t = 0$. We mentioned at the end of Section 4.1 that to evaluate the pressure $p_a(r,\theta)$ given as an integral over η of $p_a(r,\theta|\eta)$ in (4.4), we consider only sharply-peaked vorticity distributions where contributions from $\eta = 0$ dominate. At $\eta = 0$, $\kappa_t^0(k/M(\eta))_- = 0$, therefore before applying Laplace's method we must take an expansion of $\kappa_t^0(k/M(\eta_t))_-$ as $\eta \to 0$. This expansion reduces the apparent order of the first term in (7.4) by at least $O(M)$ (the true scaling will depend on how the vorticity distribution depends on k and η), thus the contribution from the scattering of the gust pressure by the trailing edge is at least $O(M)$ smaller than the leading-edge contribution to the far-field acoustics. The final term in (7.4) accounts for the rescattering of the leading-edge acoustic field by the trailing edge, and, as expected by comparison with the uniform flow case, is $O(k^{-1/2})$ smaller than the leading-edge solution.

We write the outer limit of the trailing-edge inner solution (once integrated by η_t as required in (4.4)) as

$$\frac{1}{\sqrt{kr_t}}\left(M\mathcal{P}_{t_1}(\theta_t) + \frac{1}{\sqrt{k}}\mathcal{P}_{t_2}(\theta_t)\right)\exp(\mathrm{i}kr_t\lambda_{t\,0}(\theta_t)), \tag{7.5}$$

where $\mathcal{P}_{t_2}$ is formally the same order as $\mathcal{P}_l$, but $\mathcal{P}_{t_1}$ could be smaller than $\mathcal{P}_l$ (depending on the choice of vorticity distribution). We set $\mathcal{P}_t = M\mathcal{P}_{t_1} + k^{-1/2}\mathcal{P}_{t_2}$.

7.2. *Trailing-Edge Outer Solution*

The trailing-edge outer solution is found in an identical way to the leading-edge outer solution, assuming a form

$$p_t = A_t(r_t,\theta_t)\mathrm{e}^{\mathrm{i}k\varrho_t^0(r_t,\theta_t)+\mathrm{i}k\epsilon\varrho_1^t(r_t,\theta_t)+O(\epsilon)}. \tag{7.6}$$

We find that

$$A_t(r_t,\theta_t) = D_t(\theta)(kr_t)^{-1/2}, \qquad \varrho_t^0(r_t,\theta_t) = r\lambda_{t\,\infty}(\theta_t), \tag{7.7}$$

where $\lambda_{t\,\infty}(\theta_t)$ is the corresponding trailing-edge function to $\lambda_\infty(\theta)$, and ϱ_t^1 is given by the corresponding trailing-edge formulation of (5.8). We match this to the trailing-edge inner solution by setting $D_t(\theta_t)$ equal to $\mathcal{P}_t(\theta_t)s_t(r_t,\theta_t)$, where the first factor arises from the directivity emerging from the inner region in (7.4) and the second factor accounts for the variation in ray tube area as the sound propagates though the shear - see equation

(5.2). The total far-field acoustic pressure emanating from the trailing edge then takes the form

$$\frac{D_t(\theta_t)}{\sqrt{kr_t}}\exp\left(\mathrm{i}kr_t\lambda_{t\,\infty}(\theta_t)+\frac{1}{2}\mathrm{i}k\epsilon\int_0^{\phi_t+\psi_t}L_t(\chi,\psi_t)d\chi\right). \tag{7.8}$$

Again, this is only valid in the far field, where the Mach number approaches M_∞.

7.3. *Total far-field solution*

The total far-field solution is obtained by summing the outer leading-edge solution, from (4.9) and (4.20) substituted into (4.4), and the outer trailing-edge solution, from (7.4) substituted into (4.4). In the far field, the coordinate transformation between leading-edge and trailing-edge polar coordinates is given by

$$r_t\approx r-(2+\alpha_t\epsilon)\cos\theta,\qquad \theta_t\approx\theta-\pi+\pi\,\mathrm{sgn}(\psi), \tag{7.9}$$

which allows the final solution to be expressed in terms of leading-edge variables (r,θ). The far-field acoustic pressure can then be written as

$$\frac{1}{\sqrt{kr}}\left(D_l(\theta)+D_t(\theta)\mathrm{e}^{\mathrm{i}k\varrho_s(r,\theta)}\right)\mathrm{e}^{\mathrm{i}kr\lambda_\infty(\theta)+\frac{1}{2}\mathrm{i}k\epsilon\int_0^{\phi+\psi}L(\chi,\psi)d\chi}, \tag{7.10}$$

where $D_{l,t}$ are defined in (5.9) and (7.8). In the far field, the leading- and trailing-edge ray fields interact with a phase shift

$$k\varrho_s(r,\theta)=k(\varrho_t^0(r_t,\theta_t)+\epsilon\varrho_t^1(r_t,\theta_t)-\varrho^0(r,\theta)-\epsilon\varrho^1(r,\theta)). \tag{7.11}$$

The contribution to the phase shift given by the difference between the leading-order leading- and trailing-edge far-field phase terms is

$$k(\varrho_t^0(r_t,\theta_t)-\varrho^0(r,\theta))=-(2+\alpha_t)k\lambda_\infty(\theta)\cos\theta \tag{7.12}$$

in the far field. The $O(\epsilon k)$ phase shift term, given by $\epsilon k(\varrho_t^1-\varrho^1)$, is approximated by

$$\frac{\epsilon k}{2}\int_0^2 L(\chi,\psi)d\chi \tag{7.13}$$

in the far field. Numerically integrating (7.13) for the cases we choose in the following section, we find that this contribution is only non-negligible close to $\theta=0$ or π. Since the directivity function close to $\theta=0,\pi$ is small we shall not include (7.13) in our final computed results.

8. Results

In this section we present results for the far-field pressure generated by gust-aerofoil interaction in steady shear flow. We define the far field as being a distance, r, far enough away from the aerofoil so that the mean flow is approximately uniform, and amplitude terms of $O(1/r)$ are negligible compared to the $O(1/\sqrt{r})$ terms retained in the asymptotic solution. Since there is no Rayleigh distance for this gust-aerofoil problem (because no Fresnel regions are present), we choose $r=25$ in all of the following results to illustrate the far-field behaviour. We choose non-dimensional frequency $k=10$ throughout, which is close to the peak frequency in the turbulent jet-plate interaction experiment of Davis & Pan (1993, Fig. 3). Dimensionally, $k=10$ corresponds in air to a frequency of about 2.2kHz for a chord of $0.5m$, which is in the range of practical interest. The analysis presented so far is applicable to a general thin uncambered aerofoil, and, subject to the restrictions described in Section 3, to a general mean shear distribution. For definiteness,

we now consider a gust interacting with a symmetric Joukowski aerofoil of thickness $\epsilon \ll 1$ and chord length 2 in a steady Gaussian shear flow defined by

$$U_0(y) = (\mathcal{U}_0 - 1)e^{-y^2} + 1. \tag{8.1}$$

The streamfunction for this parallel shear flow, $\psi^0(y)$ say, is simply

$$\psi^0(y) = (\mathcal{U}_0 - 1)\frac{\sqrt{\pi}}{2}\mathrm{erf}(y) + y, \tag{8.2}$$

and let $\epsilon\psi^1(x, y)$ be the perturbation to the streamfunction caused by the presence of the thin Joukowski aerofoil. We first note that in our limit of low Mach number flow the effects of compressibility on $\epsilon\psi^1(x, y)$ do not arise to the order considered, and we can therefore use the work of Sowyrda (1958), who considered the steady flow round an aerofoil in incompressible shear flow. It is then straightforward to show that, close to the leading edge of the Joukowski aerofoil,

$$\epsilon\psi^1(y) \sim \epsilon\mathcal{U}_0\left(\frac{1}{2r^2}\sin 2\theta - \frac{1}{r}\sin\theta\right) + O(\epsilon^3, \epsilon M_0), \tag{8.3}$$

while in the far field $\epsilon\psi^1(y) \to 0$. An integral expression for $\epsilon\psi^1(y)$ at arbitrary positions can also be found from Sowyrda (1958), but is not required here.

In Figure 2 we consider the effect of altering the strength of the mean shear, characterised via the parameter $S = (M_\infty - M_0)/M_\infty$, on the leading-edge directivity. Here we set $\epsilon = 0$, so that the aerofoil reduces to a flat plate, and plot the quantity $|D_l(\theta)|$ as defined in equation (5.9). When $S = 0$ the directivity pattern takes the familiar form $\cos\theta/2$, which is characteristic of low Mach number uniform flow. Varying S away from zero has a significant effect; when the shear is jet-like ($S < 0$) the directivity is particularly reduced in the downstream direction, with little effect upstream, whereas for wake-like shear ($S > 0$) the directivity is reduced predominantly upstream. Mathematically, these directivity effects may be coming from two places; first, in (4.9) through the terms dependent on β_0; and second, from the ray-tube area scaling factor $s(r, \theta)$ in (5.1). We have investigated the relative effects of both sets of terms, and have found that the directivity variations seen in Figure 2 are arising primarily from the second effect of the shear increasing the ray tube area (and therefore decreasing the pressure amplitude along the ray) in the downstream/upstream directions for S positive and negative respectively. In this case, the effect of varying S on the form of the incident gust being scattered, as contained within the terms in (4.9), has less impact on the leading-edge directivity.

In Figure 3 the effects of aerofoil thickness on the leading-edge directivity are considered. For the case of very low mean shear, $S = 0.033$, the $\cos\theta/2$ directivity seen in Figure 2 is regained in each case. The pressure amplitude increases as thickness increases, which not surprisingly is consistent with the results of Tsai (1992), who considered uniform mean flow. In contrast, for the case of more significant shear, $S = 0.333$, increasing the thickness from zero actually changes the shape of the directivity. The leading-edge sound is made up of two contributions; the leading-order term corresponding to flat-plate scattering, see (4.9), and an additive correction term of relative size $O(\epsilon\sqrt{k})$ to account for the effects of thickness in the leading-edge region, see (4.20). The interference between these two sources in shear gives rise to the lobular directivity pattern seen in Figure 3b. Note that the contribution from (4.20) takes the same form as the contribution from (4.9), but with a multiplicative correction factor which involves several effects (see the brief discussion following (4.20)). However, the variation with observer angle θ seen in Figure 3b can only arise from the term in this correction factor involving $d(k\beta_0, k\psi)$, which in turn arises from the term on the right hand side of equation (2.9), i.e. from the

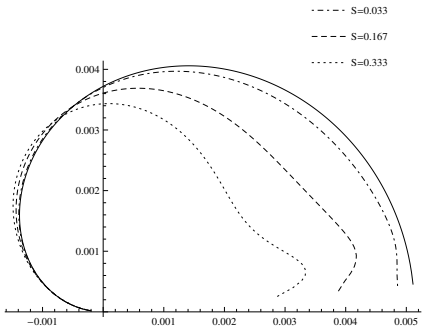

(a) Positive S, with $M_\infty = 0.3$.

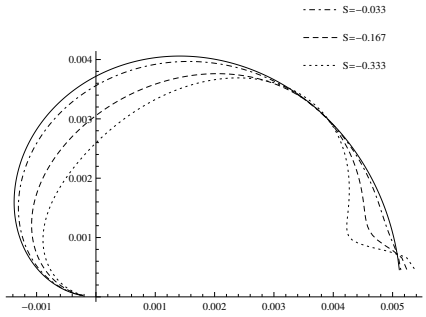

(b) Negative S, with $M_0 = 0.3$.

Figure 2: Leading-edge far-field acoustic pressure generated by gust-aerofoil interaction in a background steady parallel flow around a flat plate, $\epsilon = 0$, with $k = 10$ and varying strengths of shear, S.

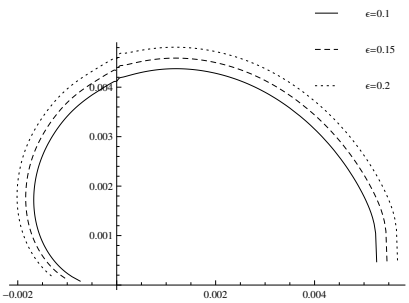

(a) $M_0 = 0.29$, $M_\infty = 0.3$, $S = 0.033$.

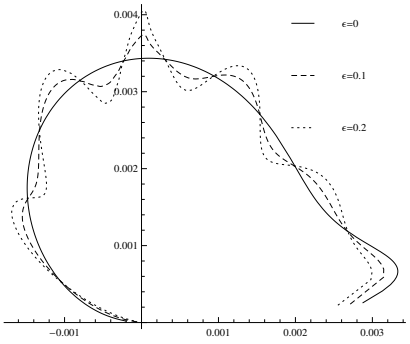

(b) $M_0 = 0.2$, $M_\infty = 0.3$, $S = 0.333$.

Figure 3: Leading-edge far-field acoustic pressure generated by gust-aerofoil interaction in background shear flows with $k = 10$, around Joukowski aerofoils of varying thickness, denoted by ϵ.

interaction between the leading-order scattered field and the non-uniformity of the mean shear flow near the leading edge. We stress that this interference within the leading-edge field is only present in shear flow.

We must choose an upstream vorticity distribution in order to obtain quantitative results for the trailing-edge term, $\mathcal{P}_{t_1}$, in (7.5). We therefore choose the vorticity to be $\tilde{\Omega} \sim \mathrm{e}^{-k\eta^2}$. In Figure 4 we see the relative effects of the two interactions which make up the sound emanating from the trailing edge of the aerofoil. These two terms are given by $M\mathcal{P}_{t_1}$ and $k^{-1/2}\mathcal{P}_{t_2}$ in (7.5). The latter term describes the sound reaching the observer via the rescattering of the leading-edge field by the trailing edge and is familiar, as it is the primary component of trailing-edge noise in uniform flow gust-aerofoil interaction. However, the scattering of the pressure associated with the gust by the trailing edge (the first term) is peculiar to shear flow interactions (since in zero mean shear the gust is pressure-free), and as we see in Figure 4 has a non-negligible effect on the total trailing-edge contribution upstream of the aerofoil. For our chosen vorticity distribution, $M\mathcal{P}_{t_1}$ is

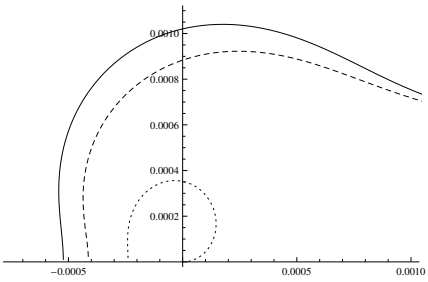

Figure 4: Trailing-edge far-field pressure generated by gust-aerofoil interaction in background shear flow around a Joukowski aerofoil with $S = 0.333$, $k = 10$, $\epsilon = 0.1$. The solid line denotes the total trailing-edge directivity. The dashed line denotes the contribution from the rescattering of the leading-edge field by the trailing edge, and the dotted line denotes scattering by the trailing-edge of pressure associated with the gust.

$O(k^{-1/4})$ smaller than $k^{-1/2}\mathcal{P}_{t_2}$ in the upstream region. Downstream of the aerofoil the effect is diminished, since the acoustic field from the scattering of the gust pressure by the trailing edge has the characteristic $\sin\theta/2$ type directivity pattern. The two components of trailing-edge sound could in principle interfere, as was seen at the leading edge in Figure 3b. However, modulation of the trailing-edge directivity is not observed in Figure 4 due to the disparity between the relative magnitudes of the two components.

We now consider the total scattered acoustic pressure as the sum of leading- and trailing-edge fields. In Figure 5 we consider the far-field pressure in the two very low shear cases $S = \pm 0.033$ for the flat plate, $\epsilon = 0$. The significant modulation of the directivity is now caused by the interference between the leading- and trailing-edge fields, and is of course absent in the comparable plots of just the leading-edge flat-plate field (see Figure 2). We repeat these flat-plate calculations in Figure 6, but now with significant shear, and similar directivity patterns are again observed. Note that positive shear significantly increases/decreases the sound level in the upstream/downstream directions respectively, and vice versa for negative shear. This effect cannot be explained by simple ray tracing arguments, which would suggest that rays in positive/negative shear flow would tend to bend in the direction of decreasing/increasing θ, see Amiet (1978). Rather, changing the shear flow is changing the phase shift, (7.12), between the leading- and trailing-edge fields, which in turns changes the interference pattern observed in the far field.

In Figure 7 we again consider the total far-field scattered pressure but now introduce non-zero thickness in the case of significant shear, $S = 0.333$. We see that the aerofoil thickness has a strong effect on the directivity shape in the forward arc. In particular, for $\epsilon = 0.2$ note how the lobes labelled A,B,C,D have markedly differing amplitudes (for instance, the relatively strong lobes A and C are separated by less pronounced lobes B and D). This is in contrast to the case of zero thickness, where it can be seen that the amplitude of the lobes in the forward arc are quite similar to each other. This change in behaviour has arisen from the interference between the components of the leading-edge source, as identified in Figure 3b: for zero thickness the far-field directivity is determined by the interference between two sources, one at the leading edge and one at the trailing edge, which leads to interference fringes of comparable size. In contrast, inclusion of the third source (the thickness-related source at the leading edge) modulates these interference fringes, leading to the modulated pattern of lobes observed in Figure 7.

In Figure 8 we vary the strength of the mean shear S by varying M_∞ while fixing

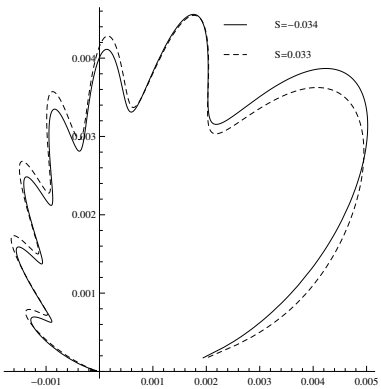

Figure 5: Far-field pressure at $r = 25$ generated by gust-aerofoil interaction in almost uniform Gaussian shear flow, $M \approx 0.3$, $k = 10$, and $\epsilon = 0$.

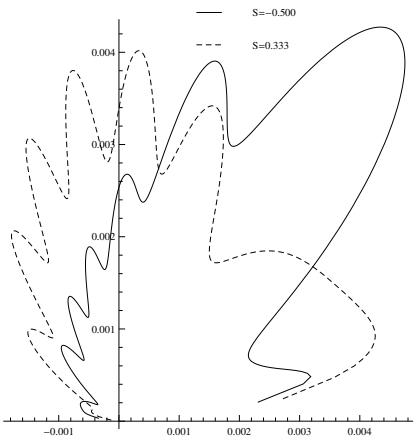

Figure 6: Far-field pressure at $r = 25$ generated by gust-aerofoil interaction in jet-like and wake-like shear flows, at $k = 10$, and $\epsilon = 0$.

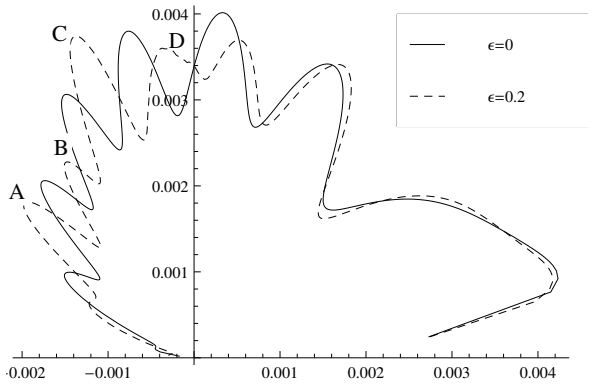

Figure 7: Far-field pressure at $r = 25$ generated by gust-aerofoil interaction in Gaussian shear flows with $M_0 = 0.2$, $M_\infty = 0.3$ ($S = 0.333$), and $k = 10$. Thickness is varied.

M_0, and see that the directivity is again significantly affected. One key effect here is the variation of the ray-tube area, as in Figure 2, but a second effect arises, just as in Figure 7, from the additional interference effect between the leading-edge sources (recall from the discussion of Figure 3 that there is no mutual interference between the leading-edge sources in the absence of mean shear). The angular position of the lobes changes as we vary S, due to the variation of M_∞; the location of the lobes is determined mainly by the phase differences between waves travelling from the leading and trailing edges, which is strongly dependent on the Mach number at infinity.

Finally, Figure 9 illustrates the effect of shear strength on the total sound power in the far field (i.e. the sound power integrated over all observer angles). For each thickness, the

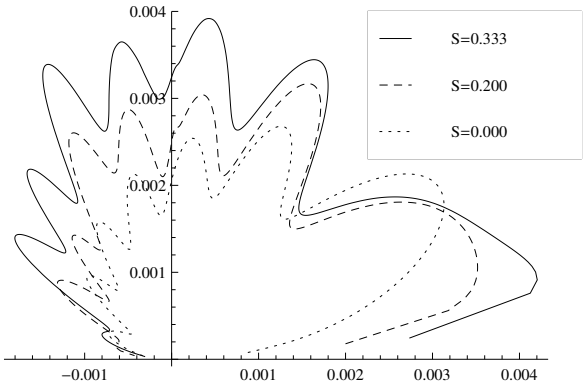

Figure 8: Far-field pressure at $r = 25$ generated by gust-aerofoil interaction in Gaussian shear flow with $M_0 = 0.2$, $k = 10$, $\epsilon = 0.1$ and varying S.

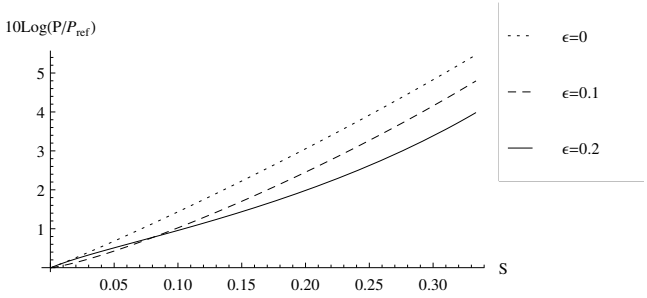

Figure 9: Normalised total sound power, $10\log(P)$, versus shear strength, S, for varying aerofoil thickness, with $k = 10$ and $M_0 = 0.2$. Each result is normalised by the power produced in uniform flow (i.e. $S = 0$) for the given aerofoil thickness.

sound power increases with shear strength, since an increase in shear strength increases the self-noise component of the unsteady flow. Once in moderate shear flow, the increase in power for thicker aerofoils is lower than the increase in power for thinner aerofoils, illustrating that the consequence of a strong non-uniform steady flow around the nose of an aerofoil is to reduce the effectiveness of the self-noise component of the scattered acoustics (recall, Figure 3b has also shown that the non-uniform flow around the nose has a significant effect on the self-noise component). At low shear strength, however, we see a different dependence of power level on thickness. This is due to the additional competing effect of stronger gust mean-flow interaction near the nose for thicker aerofoils. We believe that the key point to be taken away from Figure 9 is that significant mean shear can increase the power level by up to 5 decibels, confirming the need for inclusion of shear in our analysis.

9. Conclusions

We have constructed a model for the sound generated by gust-aerofoil interaction in background parallel shear flow, using asymptotic analysis in the limits of large gust frequency, k, and small but non-zero aerofoil thickness and Mach number. We have determined the first two terms in both the amplitude and the phase of the scattered pressure in the far field. Our key finding is that including mean shear has a significant effect, of up to 5 decibels, on the power level, compared to the uniform flow case (Figure 9).

In uniform mean flow, as studied by Myers & Kerschen (1997) and Tsai (1992), the sound is dominated by the interaction of the gust with the leading edge of the aerofoil and the scattering of the leading-edge acoustic field by the trailing edge, with the latter being formally $O(k^{-1/2})$ smaller than the former. We have shown that this feature is also present in shear flow, but that in addition the trailing edge itself acts as a noise source, as it scatters the hydrodynamic pressure associated with the gust into out-going acoustic waves propagating to infinity. This trailing-edge noise is formally the same order in k as the leading-edge noise, but in practice we found it to be significantly smaller, although it is certainly non-negligible.

We have not presented results for varying k, since this does not seem to introduce new features; as in the case of uniform flow, increasing k within our high-frequency regime reduces the acoustic amplitude and increases the number of lobes in the directivity. We use the preferred limit $\epsilon k = O(1)$; the very high frequency limit in therefore included within this, provided we send the thickness to zero. The low frequency regime is not covered at all, however in that case the aerofoil would become compact and one would expect the shear effects to be much reduced.

We have seen that changing the shear flow can have a strong effect on the directivity. This is evident in Figure 6, where we plot the far-field pressure for a zero-thickness aerofoil for jet-like and wake-like shear. The lobed directivity pattern arises from the phase shift associated with the differing paths from the leading and trailing edges to the observer, and by changing the shear one can make significant changes to this phase shift and hence to the interference pattern in the far field. We have calculated the first two terms (specifically $O(k)$ and $O(1)$) in the phase of the leading- and trailing-edge components, and therefore effectively the first two terms in the phase shift between them. Changing the shear base flow in fact changes the leading-order phase term, and therefore has a more significant effect, as witnessed in Figure 6, than for instance changing the aerofoil geometry, which will only affect the second-order phase term. The shear width has not been varied in the presented results; the key parameter is really the shear amplitude, S, measuring the relative shear between the aerofoil surface and the mean flow at infinity, and we have seen that changing S does have a significant effect.

In addition, we have identified another mechanism by which the shear modifies the directivity, this time associated with the aerofoil thickness. This involves two stages. First, the leading-order field from the leading edge (which is caused by the momentum-blocking of the incident gust by the aerofoil surface) and the second-order field from the leading edge (which is $O(\epsilon\sqrt{k})$ smaller than the leading-order term and is caused by the interaction between the unsteady flow and the non-uniform mean flow close to the thick leading edge) interfere with each other (see Figure 3b). Second, this total leading-edge field interferes with the trailing-edge field to produce a modulated far-field directivity, see Figure

7. This effect is not present in zero shear, because in that case the two components of the leading-edge field are in phase with each other, and the first stage of the interference does not occur.

Our theory holds for more complicated parallel shear flows than the symmetric, single maximum/minimum case presented here, but in that case more extensive analytical and numerical calculations would have to be included in order to produce the far-field scattered sound pressure. Similarly, it would also be possibly to consider asymmetric aerofoils by including the effects of angle of attack and camber on the mean flow, the gust evolution and the sound generation, but again significant additional complexity would be introduced. The issue of extending our work to $O(1)$ subsonic Mach numbers, however, seems much more difficult, not least because the small Mach number limit has allowed us to complete asymptotic calculations which otherwise appeared intractable at various points. Even so, we believe that the physical insights we have derived have broad application in a range of areas. We are not aware of any fully-computational approaches to this problem, but given the experience of gust-aerofoil interaction in uniform flow we believe that our approach would provide a useful complement to fully numerical computations in the high-frequency regime.

The work in this paper was funded by EPSRC under grant EP/I010440/1. We are very grateful for this support.

Appendix A

The first two terms in the transverse component of the gust velocity, $v_g(\phi,\psi) = v_g^0(\phi,\psi) + \epsilon\sqrt{k}v_g^1(\phi,\psi) + O(\epsilon)$, are given by

$$v_g^0(\phi,\psi) = \int_{\psi}^{\infty} \mathrm{e}^{\mathrm{i}k\phi/M(\eta)}\tilde{\Omega}(\eta)\left[\frac{V_1^0(k/M(\eta),\psi)}{U_1^0(k/M(\eta),\eta)} - \frac{\gamma^0(\eta)V_{\mathrm{out}}^0(k/M(\eta),\psi)}{U_1^0(k/M(\eta),\eta)}\right]d\eta$$
$$- \int_{-\infty}^{\psi} \mathrm{e}^{\mathrm{i}k\phi/M(\eta)}\tilde{\Omega}(\eta)\frac{\gamma^0(\eta)V_{\mathrm{out}}^0(k/M(\eta),\psi)}{U_1^0(k/M(\eta),\eta)}d\eta, \qquad (\mathrm{A}\,1a)$$

$$v_g^1(\phi,\psi) = \int_{\psi}^{\infty} \frac{\mathrm{e}^{\mathrm{i}k\phi/M(\eta)}\tilde{\Omega}(\eta)}{U_1^0(k/M(\eta),\eta)}\Big[V_1^1(k/M(\eta),\psi) - \gamma^1(\eta)V_{\mathrm{out}}^0(k/M(\eta),\psi) - \gamma^0(\eta)V_{\mathrm{out}}^1(k/M(\eta),\psi)$$
$$- U_1^1(k/M(\eta),\eta)\Big(V_1^0(k/M(\eta),\psi) - \gamma^0(\eta)V_{\mathrm{out}}^0(k/M(\eta),\psi)\Big)\Big]d\eta$$
$$- \int_{-\infty}^{\psi} \frac{\mathrm{e}^{\mathrm{i}k\phi/M(\eta)}\tilde{\Omega}(\eta)}{U_1^0(k/M(\eta),\eta)}\Big[\gamma^1(\eta)V_{\mathrm{out}}^0(k/M(\eta),\psi) + \gamma^0(\eta)V_{\mathrm{out}}^1(k/M(\eta),\psi)$$
$$-\gamma^0(\eta)V_{\mathrm{out}}^0(k/M(\eta),\psi)\frac{U_1^1(k/M(\eta),\eta)}{U_1^0(k/M(\eta),\eta)}\Big]d\eta, \qquad (\mathrm{A}\,1b)$$

for $\psi > 0$.

The acoustic pressure generated at the leading edge is found from (4.4), using

$$p_a^0(\Phi,\Psi|\eta) = \mathrm{sgn}(\Psi)\frac{\tilde{\Omega}(\eta)\tilde{Q}^0(\eta)M(\eta)}{2\pi\mathrm{i}}\int_{-\infty}^{\infty}\frac{\mathrm{e}^{\mathrm{i}\alpha\Phi/k}\kappa^0(k/M(\eta))_+P_{\mathrm{out}}^0(\alpha,|\Psi|/k)}{(k-\alpha M(\eta))\kappa^0(\alpha)_+V_{\mathrm{out}}^0(\alpha,0_+)}d\alpha, \qquad (\mathrm{A}\,2a)$$

$$p_a^1(\Phi,\Psi|\eta) = \mathrm{sgn}(\Psi)\frac{\tilde{\Omega}(\eta)\tilde{Q}^0(\eta)M(\eta)}{2\pi \mathrm{i}}\int_{-\infty}^{\infty}\frac{\mathrm{e}^{\mathrm{i}\alpha\Phi/k}\kappa^0(k/M(\eta))_+P^1_{\mathrm{out}}(\alpha,|\Psi|/k)}{(k-\alpha M(\eta))\kappa^0(\alpha)_+V^0_{\mathrm{out}}(\alpha,0_+)}d\alpha$$
$$+\mathrm{sgn}(\Psi)\frac{\tilde{\Omega}(\eta)\tilde{Q}^1(\eta)M(\eta)}{2\pi \mathrm{i}}\int_{-\infty}^{\infty}\frac{\mathrm{e}^{\mathrm{i}\alpha\Phi/k}P^0_{\mathrm{out}}(\alpha,|\Psi|/k)\kappa^0(k/M(\eta))_+}{(k-\alpha M(\eta))\kappa^0(\alpha)_+V^0_{\mathrm{out}}(\alpha,0_+)}d\alpha$$
$$-\mathrm{sgn}(\Psi)\frac{\tilde{\Omega}(\eta)\tilde{Q}^0(\eta)M(\eta)}{2\pi \mathrm{i}}\int_{-\infty}^{\infty}\frac{\mathrm{e}^{\mathrm{i}\alpha\Phi/k}P^0_{\mathrm{out}}(\alpha,|\Psi|/k)\kappa^0(k/M(\eta))_+}{(k-\alpha M(\eta))\kappa^0(\alpha)_+V^0_{\mathrm{out}}(\alpha,0_+)}\frac{P^1_{\mathrm{out}}(\alpha,0)}{P^0_{\mathrm{out}}(\alpha,0)}d\alpha$$
$$+\mathrm{sgn}(\Psi)\frac{kM'(\eta)G^0(k/M(\eta))_-}{2\pi \mathrm{i}M(\eta)}\left(\frac{P^1_{\mathrm{out}}(k/M(\eta),0)}{P^0_{\mathrm{out}}(k/M(\eta),0)}-\frac{V^1_{\mathrm{out}}(k/M(\eta),0)}{V^0_{\mathrm{out}}(k/M(\eta),0)}\right)$$
$$\int_{-\infty}^{\infty}\frac{\mathrm{e}^{\mathrm{i}\alpha\Phi/k}P^0_{\mathrm{out}}(\alpha,|\Psi|/k)}{(k-\alpha M(\eta))\kappa^0(\alpha)_+V^0_{\mathrm{out}}(\alpha,0_+)}d\alpha. \tag{A 2b}$$

The term $p_a^0(\Phi,\Psi|\eta)$ arises from the blocking of the incident transverse gust velocity by the solid body, whilst the terms in $p_a^1(\Phi,\Psi|\eta)$ are effects of thickness; the first term in (A 2b) occurs due to the gust interacting with the steady perturbation flow around the nose of the aerofoil, the second term arises from the blocking of the chord-wise gust velocity, and the third and final terms arise from the distortion of the sound generated at the leading edge, $p_a^0(\Phi,\Psi|\eta)$, by the non-uniform flow around the nose of the aerofoil. The $\tilde{Q}^{0,1}$ are defined in (B 14) below.

Appendix B

From (4.3) we know that $A(\alpha)P_{\mathrm{out}}(\alpha,0)$ is analytic in the lower half α plane. Denote such a function by a $_-$ suffix, i.e. $A(\alpha)P_{\mathrm{out}}(\alpha,0) = [A(\alpha)P_{\mathrm{out}}(\alpha,0)]_-$. If we take an arbitrary minus function, $\kappa(\alpha)_-$, then

$$A(\alpha)P_{\mathrm{out}}(\alpha,0)\kappa(\alpha)_- = [A(\alpha)P_{\mathrm{out}}(\alpha,0)\kappa(\alpha)_-]_- = G(\alpha)_-. \tag{B 1}$$

We demand that $\kappa(\alpha)_-$ has algebraic behaviour at infinity, and that $G(\alpha)_\pm$ vanishes at infinity. As before denote the $O(1)$ term of any function by a superscript ^{0} and the $O(\epsilon\sqrt{k})$ term by a superscript ^{1}.

Define

$$F(\alpha)_- = -\frac{1}{2\pi k}\int_0^\infty \mathrm{e}^{-\mathrm{i}\alpha\Phi/k}v_g(\Phi/k,0)d\Phi = F^0(\alpha)_- + \epsilon\sqrt{k}F^1(\alpha)_-, \tag{B 2}$$

so

$$A(\alpha)V_{\mathrm{out}}(\alpha,0) = F(\alpha)_- + F(\alpha)_+, \tag{B 3}$$

where $F(\alpha)_+$ is analytic in the upper half α plane, and is unknown. Expanding (B 1) and (B 3) to $O(\epsilon\sqrt{k})$ and equating at each power yields

$$P^0_{\mathrm{out}}(\alpha,0)\kappa^0(\alpha)_-A^0(\alpha) = G^0(\alpha)_-, \tag{B 4a}$$
$$A^0(\alpha)V^0_{\mathrm{out}}(\alpha,0) = F^0(\alpha)_- + F^0(\alpha)_+, \tag{B 4b}$$

to leading order, and

$$P^0_{\mathrm{out}}(\alpha,0)\left[\kappa^1(\alpha)_-A^0(\alpha)+\kappa^0(\alpha)_-A^1(\alpha)\right] + P^1_{\mathrm{out}}(\alpha,0)\kappa^0(\alpha)_-A^0(\alpha) = G^1(\alpha)_-, \tag{B 4c}$$
$$A^1(\alpha)V_{\mathrm{out}}(\alpha,0) + A^0(\alpha)V^1_{\mathrm{out}}(\alpha,0) = F^1(\alpha)_- + F^1(\alpha)_+, \tag{B 4d}$$

to $O(\epsilon\sqrt{k})$. By demanding that $\kappa^0(\alpha)_-$ satisfies

$$\frac{P^0_{\rm out}(\alpha,0)}{V^0_{\rm out}(\alpha,0)} = \frac{\kappa^0(\alpha)_+}{\kappa^0(\alpha)_-}, \tag{B 5}$$

we find that

$$G^0(\alpha)_- = \left[F^0(\alpha)_-\kappa^0(\alpha)_+\right]_-. \tag{B 6}$$

This determines $G^0(\alpha)_-$ and also $\kappa^0(\alpha)_-$ from known quantities, P and V. Hence

$$A^0(\alpha) = \frac{G^0(\alpha)_-}{\kappa^0(\alpha)_- P_{\rm out}(\alpha,0)} \tag{B 7}$$

is determined.

To next order

$$G^0(\alpha)_-\left[\frac{P^1_{\rm out}(\alpha,0)}{P^0_{\rm out}(\alpha,0)} - \frac{V^1_{\rm out}(\alpha,0)}{V^0_{\rm out}(\alpha,0)} + \frac{\kappa^1(\alpha)_-}{\kappa^0(\alpha)_-}\right] + \kappa^0(\alpha)_+F^1(\alpha)_+ + \kappa^0(\alpha)_+F^1(\alpha)_- = G^1(\alpha)_-. \tag{B 8}$$

We are free to choose $\kappa^1(\alpha)_-$ provided we have algebraic decay at infinity. Taking the simplest case of $\kappa^1(\alpha)_- = 0$ gives

$$G^1(\alpha)_- = \left[\kappa^0(\alpha)_+F^1(\alpha)_-\right]_- + \left[G^0(\alpha)_-\left(\frac{P^1_{\rm out}(\alpha,0)}{P^0_{\rm out}(\alpha,0)} - \frac{V^1_{\rm out}(\alpha,0)}{V^0_{\rm out}(\alpha,0)}\right)\right]_-, \tag{B 9}$$

so

$$A^1(\alpha) = \frac{G^1(\alpha)_- - P^1_{\rm out}(\alpha,0)\kappa^0(\alpha)_-A^0(\alpha)}{P^0_{\rm out}(\alpha,0)\kappa^0(\alpha)_-}. \tag{B 10}$$

We see *a priori* that our condition of G vanishing at infinity is satisfied. Goldstein(ref) proves that G^0 vanishes at infinity, and hence we only require that $[\kappa^0(\alpha)_+F^1(\alpha)_-]_-$ tends to zero as $\alpha \to \infty$. This is immediate if $G^0(\alpha) \to 0$ as $\alpha \to \infty$, since F^1 will behave asymptotically in a similar way to F^0 given the form of the velocity terms $v_g^{0,1}$. We proceed using the same method as Goldstein (1978); define $R^i(\alpha)$ for $i = 0, 1$ by

$$v^i_g(\Phi/k, 0) = \int_{k/M_0}^{k/M_\infty} \mathrm{e}^{\mathrm{i}\alpha\Phi/k}\tilde{\Omega}(\eta(\alpha))R^i(\alpha)\frac{d\eta(\alpha)}{d\alpha}d\alpha, \tag{B 11}$$

and from (B 2) we see

$$F^i(\alpha)_- = \lim_{\delta\to 0_+}\frac{1}{2\pi\mathrm{i}}\int_{k/M_0}^{k/M_\infty}\frac{\tilde{\Omega}(\eta(\alpha'))}{\alpha'-\alpha+i\delta}R^i(\alpha')\frac{d\eta(\alpha')}{d\alpha'}d\alpha'. \tag{B 12}$$

Using the Plemelj formula (Ablowitz & Fokas 2003) we find

$$F^i(\alpha)_- = F^i(\alpha)_+ - (H(\alpha - k/M_0) - H(\alpha - k/M_\infty))\tilde{\Omega}(\eta(\alpha))R^i(\alpha)\frac{d\eta(\alpha)}{d\alpha}, \tag{B 13}$$

where H is the Heaviside function and the $F^i(\alpha)_+$ for $i = 0, 1$ are bounded at infinity in the upper half plane. Using (B 6) we find

$$G^0(\alpha)_- = \frac{1}{2\pi\mathrm{i}}\int_0^\infty M(\eta)\frac{\kappa^0(k/M(\eta))_+}{k-\alpha M(\eta)}\tilde{\Omega}(\eta)\tilde{Q}^0(\eta)d\eta, \tag{B 14}$$

where $\tilde{Q}^i(\eta) = R^i(k/M(\eta))$. This is the solution presented in Goldstein (1978), in which k is taken to have a small positive imaginary part to ensure convergence of all the integrals (this imaginary part is set to zero at the end of the analysis).

The solution for $G^1(\alpha)_-$ is more complicated, but is found using the same method; we have

$$G^1(\alpha)_- - G^1(\alpha)_+ = G^0(\alpha)_- \left(\frac{P^1(\alpha,0)}{P^0(\alpha,0)} - \frac{V^1(\alpha,0)}{V^0(\alpha,0)}\right) - \left(H(\alpha - k/M_0) - H(\alpha - k/M_\infty)\right)\tilde{\Omega}(\eta(\alpha))R^1(\alpha)\frac{d\eta(\alpha)}{d\alpha}, \quad \text{(B 15)}$$

so

$$G^1(\alpha)_- = \frac{1}{2\pi \mathrm{i}}\int_0^\infty M(\eta)\frac{\kappa^0(k/M(\eta))_+}{k-\alpha M(\eta)}\tilde{\Omega}(\eta)\tilde{Q}^1(\eta)d\eta + \frac{1}{2\pi\mathrm{i}}\int_0^\infty \frac{kM'(\eta)G^0(k/M(\eta))_-}{M(\eta)(k-\alpha M(\eta))}\left(\frac{P^1(k/M(\eta),0)}{P^0(k/M(\eta),0)} - \frac{V^1(k/M(\eta),0)}{V^0(k/M(\eta),0)}\right)d\eta. \quad \text{(B 16)}$$

Appendix C

Here we present the Wiener-Hopf solutions to (7.2) and (7.3). Note that we need only find $A_p(\alpha)$ correct to leading order, since the pressure jump of the leading-edge field across the aerofoil, Δp, is an order of $\sqrt{k}$ smaller than the gust velocity v_g. We have

$$p^0_{a,H}(\Phi_t,\Psi_t) = -\mathrm{sgn}(\Psi_t)\int_0^\infty \frac{\tilde{\Omega}(\eta_t)\tilde{Q}^0(\eta_t)M(\eta_t)}{2\pi\mathrm{i}} \int_{-\infty}^\infty \frac{\mathrm{e}^{\mathrm{i}\alpha\Phi_t/k}\kappa^0_t(\alpha)_- P^0_{\mathrm{out}}(\alpha,|\Psi_t|/k)}{(k-\alpha M(\eta_t))\kappa^0_t(k/M(\eta_t))_- V^0_{\mathrm{out}}(\alpha,0)}d\alpha d\eta_t, \quad \text{(C 1}a\text{)}$$

$$\begin{aligned} p^1_{a,H}(\Phi_t,\Psi_t) = &-\mathrm{sgn}(\Psi_t)\int_0^\infty \frac{\tilde{\Omega}(\eta_t)\tilde{Q}^0(\eta_t)M(\eta_t)}{2\pi\mathrm{i}}\Bigg\{ \int_{-\infty}^\infty \frac{\mathrm{e}^{\mathrm{i}\alpha\Phi_t/k}\kappa^0_t(\alpha)_- P^1_{\mathrm{out}}(\alpha,|\Psi_t|/k)}{(k-\alpha M(\eta_t))\kappa^0_t(k/M(\eta_t))_- V^0_{\mathrm{out}}(\alpha,0)}d\alpha d\eta_t \\ &- \int_{-\infty}^\infty \frac{\mathrm{e}^{\mathrm{i}\alpha\Phi_t/k}P^0_{\mathrm{out}}(\alpha,|\Psi_t|/k)\kappa^0_t(\alpha)_-}{(k-\alpha M(\eta_t))\kappa^0_t(k/M(\eta_t))_- V^0_{\mathrm{out}}(\alpha,0)}\frac{P^1_{\mathrm{out}}(\alpha,0)}{P^0_{\mathrm{out}}(\alpha,0)}d\alpha d\eta_t\Bigg\} \\ &- \mathrm{sgn}(\Psi_t)\int_0^\infty \frac{\tilde{\Omega}(\eta_t)\tilde{Q}^1(\eta_t)M(\eta_t)}{2\pi\mathrm{i}}\int_{-\infty}^\infty \frac{\mathrm{e}^{\mathrm{i}\alpha\Phi_t/k}P^0_{\mathrm{out}}(\alpha,|\Psi_t|/K)\kappa^0_t(\alpha)_-}{(k-\alpha M(\eta_t))\kappa^0_t(k/M(\eta_t))_- V^0_{\mathrm{out}}(\alpha,0)}d\alpha d\eta_t \\ &- \mathrm{sgn}(\Psi_t)\int_0^\infty \frac{kM'(\eta_t)G^0_t(k/M(\eta_t))_+}{2\pi\mathrm{i}M(\eta_t)}\left(\frac{P^1_{\mathrm{out}}(k/M(\eta_t),0)}{P^0_{\mathrm{out}}(k/M(\eta_t),0)} - \frac{V^1_{\mathrm{out}}(k/M(\eta_t),0)}{V^0_{\mathrm{out}}(k/M(\eta_t),0)}\right) \\ &\int_{-\infty}^\infty \frac{\mathrm{e}^{\mathrm{i}\alpha\Phi_t/k}P^0_{\mathrm{out}}(\alpha,|\Psi_t|/k)\kappa^0_t(\alpha)_-}{(k-\alpha M(\eta_t))\kappa^0_t(k/M(\eta_t))_- V^0_{\mathrm{out}}(\alpha,0)}d\alpha d\eta_t, \end{aligned} \quad \text{(C 1}b\text{)}$$

$$p^0_{a,p}(\Phi_t,\Psi_t) = \int_{-\infty}^\infty \mathrm{e}^{\mathrm{i}\alpha\Phi_t/k}\frac{\kappa^0_t(\alpha)_- G_{t,p}(\alpha)_-}{V^0_{\mathrm{out}}(\alpha,0)}P^0_{\mathrm{out}}(\alpha,|\Psi_t|/k)d\alpha, \quad \text{(C 1}c\text{)}$$

where

$$\kappa_t^0(\alpha)_+\kappa_t^0(\alpha)_- = \frac{V_{\text{out}}^0(\alpha,0)}{P_{\text{out}}^0(\alpha,0)}, \tag{C 2a}$$

$$G^0(\alpha)_+ = -\frac{1}{2\pi \mathrm{i}}\int_0^\infty \frac{M(\eta_t)\tilde{\Omega}(\eta_t)\tilde{Q}(\eta_t)}{(k-\alpha M(\eta_t))\kappa_t^0(k/M(\eta_t))_-}d\eta_t, \tag{C 2b}$$

$$G_{t,p}(\alpha)_- = \left[\kappa_t^0(\alpha)_+ F_t(\alpha)_-\right]_-, \tag{C 2c}$$

$$F_t(\alpha)_- = -\frac{1}{2\pi k}\int_0^\infty \Delta p(\Phi_t/k)\mathrm{e}^{-\mathrm{i}\alpha\Phi_t/k}d\Phi_t. \tag{C 2d}$$

Here η_t is the trailing-edge version of the variable η given in (3.5).

REFERENCES

Ablowitz, M. J. & Fokas, A. S. *Complex Variables: Introduction and Applications*. Cambridge University Press, 2003.

Allampalli, V., Hixon, R., Nallasamy, M. & Sawyer, S. D. High-accuracy large-step explicit Runge-Kutta (HALE-RK) schemes for computational aeroacoustics. *Journal of Computational Physics* **228**, 3837–3850, 2009.

Amiet, R.K. Refraction of sound by a shear layer. *Journal of Sound and Vibration* **58**, 467–482, 1978.

Atassi, H. M. & Grzedzinski, J. Unsteady disturbances of streaming motions around bodies. *Journal of Fluid Mechanics* **209**, 385–403, 1989.

Ayton, L. J. & Peake, N. On high-frequency noise scattering by aerofoils in flow. *Journal of Fluid Mechanics* **734**, 144–182, 2013.

Batchelor, G. K. *An Introduction to Fluid Dyanmics*. Cambridge University Press, 1967.

Bender, C. M. & Orszag, S. A. *Advanced Mathematical Methods for Scientists and Engineers*. Springer, 1978.

Bodony, D. J. Scattering of an entropy disturbance into sound by a symmetric thin body. *Physics of Fluids* **21**, 096101, 2009.

Davis, M. R., & Pan, N. H. Noise generated by a turbulent jet interacting with a rigid plate. *Journal of Sound and Vibration* **167**, 165–181, 1993.

Durbin, P. A. High frequency Green function for aerodynamic noise in moving media, part I; general theory. *Journal of Sound and Vibration* **91**, 519–525, 1983.

Finnigan, J. J. A streamline coordinate system for distorted two-dimensional shear flows. *Journal of Fluid Mechanics* **130**, 241–258, 1983.

Goldstein, M. E. Unsteady vortical and entropic distortions of potential flows round arbitrary obstacles. *Journal of Fluid Mechanics* **89**, 433–468, 1978.

Goldstein, M. E. Characteristics of the unsteady motion on transversely sheared mean flows. *Journal of Fluid Mechanics* **84**, 305–329, 1978.

Goldstein, M. E. Scattering and distortion of the unsteady motion on transversely sheared mean flows. *Journal of Fluid Mechanics* **91**, 601–632, 1979.

Goldstein, M. E., Afsar, M. Z., & Leib, S. J. Non-homogeneous rapid distortion theory on transversely sheared mean flows. *Journal of Fluid Mechanics* **736**, 532–569, 2013.

Hixon, R., Scott, J. R., Sawyer, S. & Nallasamy, M. Application of a nonlinear computational aeroacoustics code to the gust-airfoil problem. *AIAA Journal* **44**, 323–328, 2006.

Mengle, V. G., Stoker, R. W., Brusniak, L., Elkoby, R. & Thomas, R. H. Flaperon Modification Effect on Jet-Flap Interaction Noise Reduction for Chevron Nozzles. 13th AIAA/CEAS Aeroacoustics Conference, May 21–23, AIAA–2007–3666, 2007.

Myers, M. R. & Kerschen, E. J. Influence of incidence angle on sound generation by airfoils interacting with high-frequency gusts. *Journal of Fluid Mechanics* **292**, 271–304, 1995.

Myers, M. R. & Kerschen, E. J. Influence of camber on sound generation by airfoils interacting with high-frequency gusts. *Journal of Fluid Mechanics* **353**, 221–259, 1997.

Noble, B. *Methods Based on the Wiener-Hopf Technique for the Solution of Partial Differential Equations*. Chelsea Publications, 1998.

Peake, N. & Kerschen, E. J. Influence of mean loading on noise generated by the interaction of gusts with a flat-plate cascade: upstream radiation. *Journal of Fluid Mechanics* **347**, 315–346, 1997.

Peake, N. & Kerschen, E. J. Influence of mean loading on noise generated by the interaction of gusts with a cascade: downstream radiation. *Journal of Fluid Mechanics* **515**, 99–133, 2004.

Peake, N. & Parry, A. B. Modern challenges facing turbomachinery aeroacoustics. *Annual Review of Fluid Mechanics* **44**, 227–248, 2012.

Semiletov, V., Karabasov, S., Lyubimov, D., Faranosov, G. & Kopiev, V. On the effect of flap deflection on jet flow for a jet-pylon-wing configuration: near-field and acoustic modelling results. 19th AIAA/CEAS Conference, Berlin 27–29 May, AIAA–2013–2215, 2013.

Sowyrda, A. Theory of cambered Joukowsky airfoils in shear flow. *Tech. Rep.*. Cornell University, 1958.

Thwaites, B. *Incompressible aerodynamics: an account of the theory and observation of the steady flow of incompressible fluid past aerofoils, wings, and other bodies*. Dover Publications, 1960.

Tsai, C-T. Effect of Airfoil Thickness on High-Frequency Gust Interaction Noise. PhD thesis, University of Arizona, 1992.

Van Dyke, M. *Perturbation methods in fluid mechanics*. Parabolic Press, 1975.